INTERNATIONAL STANDARD

ISO 18589-7

First edition
2013-10-01

Measurement of radioactivity in the environment — Soil —

Part 7: In situ measurement of gamma-emitting radionuclides

Mesurage de la radioactivité dans l'environnement — Sol —

Partie 7: Mesurage in situ des radionucléides émetteurs gamma

Reference number
ISO 18589-7:2013(E)

ISO copyright office
Case postale 56 • CH-1211 Geneva 20
Tel. + 41 22 749 01 11
Fax + 41 22 749 09 47
E-mail copyright@iso.org
Web www.iso.org

Published in Switzerland

Contents

Page

Foreword ... **iv**

Introduction ... **v**

1 Scope ... **1**

2 Normative references ... **1**

3 Terms, definitions, symbols, and units ... **2**
3.1 Terms and definitions ... 2
3.2 Symbols and units ... 3

4 Principles ... **6**
4.1 Measurement method ... 6
4.2 Uncertainties of the measurement method ... 6

5 Equipment ... **6**
5.1 Portable ***in situ*** spectrometry system ... 6
5.2 Detector System ... 7
5.3 Pulse processing electronics ... 8
5.4 Assembly jig for a detector system ... 9
5.5 Collimated detector ... 9

6 Procedure ... **12**
6.1 Calibration ... 12
6.2 Method of combined calibrations ... 12

7 Quality assurance and quality control program ... **17**
7.1 General ... 17
7.2 Influencing variables ... 17
7.3 Instrument verification ... 17
7.4 Method verification ... 17
7.5 Quality control program ... 17
7.6 Standard operating procedure ... 19

8 Expression of results ... **19**
8.1 Calculation of activity per unit of surface area or unit of mass ... 19
8.2 Calculation of the characteristic limits and the best estimate of the measurand as well as its standard uncertainty ... 19
8.3 Calculation of the radionuclide specific ambient dose rate ... 21

9 Test report ... **22**

Annex A (informative) **Influence of radionuclides in air on the result of surface or mass activity measured by *in situ* gamma spectrometry** ... **23**

Annex B (informative) **Influence quantities** ... **24**

Annex C (informative) **Characteristics of germanium detectors** ... **27**

Annex D (informative) **Field-of-view of an *in situ* gamma spectrometer as a function of the photon energy for different radionuclide distributions in soil** ... **29**

Annex E (informative) **Methods for calculating geometry factors and angular correction factors** ... **33**

Annex F (informative) **Example for calculation of the characteristic limits as well as the best estimate of the measurand and its standard uncertainty** ... **41**

Annex G (informative) **Conversion factors for surface or mass activity to air kerma rate and ambient dose equivalent rate for different radionuclide distribution in soil** ... **45**

Annex H (informative) **Mass attenuation factors for soil and attenuation factors for air as a function of photon energy and deviation of *G(E,V)* for different soil compositions** ... **52**

Bibliography ... **54**

Foreword

ISO (the International Organization for Standardization) is a worldwide federation of national standards bodies (ISO member bodies). The work of preparing International Standards is normally carried out through ISO technical committees. Each member body interested in a subject for which a technical committee has been established has the right to be represented on that committee. International organizations, governmental and non-governmental, in liaison with ISO, also take part in the work. ISO collaborates closely with the International Electrotechnical Commission (IEC) on all matters of electrotechnical standardization.

The procedures used to develop this document and those intended for its further maintenance are described in the ISO/IEC Directives, Part 1. In particular the different approval criteria needed for the different types of ISO documents should be noted. This document was drafted in accordance with the editorial rules of the ISO/IEC Directives, Part 2. www.iso.org/directives

Attention is drawn to the possibility that some of the elements of this document may be the subject of patent rights. ISO shall not be held responsible for identifying any or all such patent rights. Details of any patent rights identified during the development of the document will be in the Introduction and/or on the ISO list of patent declarations received. www.iso.org/patents

Any trade name used in this document is information given for the convenience of users and does not constitute an endorsement.

The committee responsible for this document is ISO/TC 85, *Nuclear energy, nuclear technologies, and radiological protection*, Subcommittee SC 2, *Radiological protection*.

ISO 18589 consists of the following parts, under the general title *Measurement of the radioactivity in the environment — Soil*:

— *Part 1: General guidelines and definitions*

— *Part 2: Guidance for the selection of the sampling strategy, sampling and pre-treatment of samples*

— *Part 3: Measurements of gamma-emitting radionuclides*

— *Part 4: Measurement of plutonium isotopes (plutonium 238 and plutonium 239 + 240) by alpha spectrometry*

— *Part 5: Measurement of strontium 90*

— *Part 6: Measurement of gross alpha and gross beta activities*

— *Part 7: In situ measurement of gamma-emitting radionuclides*

Introduction

In situ gamma spectrometry is a rapid and accurate technique to assess the activity concentration of gamma-emitting radionuclides present in the top soil layer or deposited onto the soil surface. This method is also used to assess the dose rates of individual radionuclides.

In situ gamma spectrometry is a direct physical measurement of radioactivity that does not need any soil samples, thus reducing the time and cost of laboratory analysis of large number of soil samples.

The quantitative analysis of the recorded line spectra requires a suitable area for the measurement. Furthermore, it is required to know the physicochemical properties of the soil and the vertical distribution in the soil to assess the activity of the radionuclides.

Measurement of radioactivity in the environment — Soil —

Part 7: In situ measurement of gamma-emitting radionuclides

1 Scope

This part of 18589 specifies the identification of radionuclides and the measurement of their activity in soil using *in situ* gamma spectrometry with portable systems equipped with germanium or scintillation detectors.

This part of ISO 18589 is suitable to rapidly assess the activity of artificial and natural radionuclides deposited on or present in soil layers of large areas of a site under investigation.

This part of ISO 18589 can be used in connection with radionuclide measurements of soil samples in the laboratory (ISO 18589-3) in the following cases:

— routine surveillance of the impact of radioactivity released from nuclear installations or of the evolution of radioactivity in the region;

— investigations of accident and incident situations;

— planning and surveillance of remedial action;

— decommissioning of installations or the clearance of materials.

It can also be used for the identification of airborne artificial radionuclides, when assessing the exposure levels inside buildings or during waste disposal operations.

Following a nuclear accident, *in situ* gamma spectrometry is a powerful method for rapid evaluation of the gamma activity deposited onto the soil surface as well as the surficial contamination of flat objects.

NOTE The method described in this part of ISO 18589 is not suitable when the spatial distribution of the radionuclides in the environment is not precisely known (influence quantities, unknown distribution in soil) or in situations with very high photon flux. However, the use of small volume detectors with suitable electronics allows measurements to be performed under high photon flux.

2 Normative references

The following documents, in whole or in part, are normatively referenced in this document and are indispensable for its application. For dated references, only the edition cited applies. For undated references, the latest edition of the referenced document (including any amendments) applies.

ISO/IEC 17025, *General requirements for the competence of testing and calibration laboratories*

IEC 61275, *Radiation protection instrumentation — Measurement of discrete radionuclides in the environment — In situ photon spectrometry system using a germanium detector*

ISO 11929, *Determination of the characteristic limits (decision threshold, detection limit and limits of the confidence interval) for measurements of ionizing radiation — Fundamentals and application*

3 Terms, definitions, symbols, and units

3.1 Terms and definitions

For the purposes of this document, the following terms and definitions apply.

3.1.1
intrinsic efficiency
η_0
cross section of a detector for photons from the direction of the crystal symmetry axis

Note 1 to entry: The intrinsic efficiency depends on the energy of the photon.

3.1.2
detector efficiency
$\eta_0(E)$
detector efficiency in the direction of the crystal symmetry axis as a function of the photon energy E

3.1.3
detector height
d
distance between the geometrical centre of the crystal and the soil surface

3.1.4
efficiency per unit of surface area or unit of mass
ε
ratio between the net count rate of an absorption line with energy E and the photon emission rate per unit area or mass

3.1.5
relative detection efficiency
ratio, expressed in percentage, of the count rate in the ^{60}Co 1 333 keV total absorption peak to the one obtained with a 3 x 3 inch NaI(Tl) scintillator for normal incidence and at 0,25 m from the source

3.1.6
geometry factor
G
ratio between the flux density without scattered photons measured at the detector location and the photon emission rate per unit area or mass

3.1.7
aperture angle of collimator
ϑ_{col}
characteristic angle for an *in situ* gamma spectrometer with collimator

3.1.8
relaxation mass per unit area[7]
β
mathematical parameter describing radionuclide distribution as a function of soil depth

Note 1 to entry: It indicates the soil mass per unit of surface area at which gamma activity decreases to 1/e (37 %).

3.1.9
field-of-view of a detector
soil surface area, from which 90 % of the unscattered detected photons originate

3.1.10
distribution model
V
entity of all physical and geometrical parameters to describe the distribution of the radionuclide in the environment as well as the interaction of an emitted photon with soil and air

3.1.11
angular coefficient
k_m
factor taking into account the angular response of the detector and the angular distribution of the incident flux

3.1.12
measurement area
area in the soil and/or on the soil surface having radionuclide activity per unit of surface area or unit of mass

3.1.13
mass per unit area (collimator)[7]
ζ_{col}
product of material density and wall thickness of a collimator

Note 1 to entry: The mass per unit area is reported for a polar angle, ϑ, of 90° in relation to the crystal centre.

3.1.14
cross section of the detector
ratio of the net rate of the total absorption line at energy E and the flux density of unscattered photons of the energy E in the detector

3.1.15
calibration factor per unit of surface area or unit of mass
w
ratio of the activity of surface area or unit of mass of the radionuclide to the net count rate of the total absorption line

3.2 Symbols and units

For the purposes of this part of ISO 18589, the symbols and units defined in ISO 11929 and given in Table 1 apply.

Table 1 — Symbols

Symbols	Designation	Unit
a	Activity of a given radionuclide at the time of measurement	
	a) per unit of surface area	$Bq \cdot m^{-2}$
	b) per unit of mass	$Bq \cdot kg^{-1}$
$\hat{a}$	Best estimate of the measurand of the activity of the radionuclide in question	
	a) per unit of surface area	$Bq \cdot m^{-2}$
	b) per unit of mass	$Bq \cdot kg^{-1}$
a_K	Activity of the calibration standard at the time of measurement	Bq
a_0	Activity of the radionuclide in question at the soil surface	$Bq \cdot m^{-2}$
$a(\zeta)$	Projected surface activity as a function of mass per unit at the surface of the soil	$Bq \cdot m^{-2}$
a^*	Decision threshold of the measurand of the radionuclide in question at the time of measurement	
	a) per unit of surface area	$Bq \cdot m^{-2}$
	b) per unit of mass	$Bq \cdot kg^{-1}$
$a^\#$	Detection limit of the measurand of the radionuclide in question at the time of measurement	
	a) per unit of surface area	$Bq \cdot m^{-2}$

Table 1 *(continued)*

Symbols	Designation	Unit
	b) per unit of mass	$Bq \cdot kg^{-1}$
$a^{\triangleright}$, $a^{\triangleleft}$	Upper and lower limit of the confidence interval, respectively, of the measurand of the radionuclide in question at the time of measurement	
	a) per unit of surface area	$Bq \cdot m^{-2}$
	b) per unit of mass	$Bq \cdot kg^{-1}$
c_0, c_1, c_2	Quantities to determine the decision threshold and limit of detection	-
d	Distance between the calibration source and the geometrical centre of the crystal	m
$\dot{D}$	Ambient dose rate as air kerma rate	$Gy \cdot h^{-1}$
E	Photon energy	keV
E_1	1. order exponential integral function $E_1(\alpha) = \int_1^\infty \frac{e^{-\alpha x}}{x} dx$	-
E_2	2. order exponential integral function $E_2(\alpha) = \int_1^\infty \frac{e^{-\alpha x}}{x^2} dx$	-
f_d	Decay factor	-
f_D	Factor for converting the activity of a radionuclide to ambient dose rate as air kerma rate	
	a) per unit of surface area	$Gy \cdot m^2 \cdot h^{-1} \cdot Bq^{-1}$
	b) per unit of mass	$Gy \cdot kg \cdot h^{-1} \cdot Bq^{-1}$
$f_{\dot{H}^*(10)}$	Factor for converting the activity of a radionuclide to ambient dose equivalent rate	
	a) per unit of surface area	$Sv \cdot m^2 \cdot h^{-1} \cdot Bq^{-1}$
	b) per unit of mass	$Sv \cdot kg \cdot h^{-1} \cdot Bq^{-1}$
G	Geometry factor	
	a) per unit of surface area	-
	b) per unit of mass	$kg \cdot m^{-2}$
$G(E, V)$	Geometry function of photon energy, E, and distribution, V	
	a) per unit of surface area	-
	b) per unit of mass	$kg \cdot m^{-2}$
$\dot{H}^*(10)$	The dose equivalent rate at a point in a radiation field that would be produced by the corresponding expanded and aligned field in the ICRU sphere at a depth, d (here 10 mm), on the radius opposing the direction of the aligned field	$Sv \cdot h^{-1}$
k, $k_{1-\alpha}$, $k_{1-\beta}$, $k_{1-\gamma/2}$	Quantiles of the standardized normal distribution	-
k_m	Angular coefficient for photon irradiation from the polar angular segment, m	-
M	Number of polar angular segments	-
m	Index for polar angular segment	-
n_g	Total counts of the total absorption line	-

Table 1 *(continued)*

Symbols	Designation	Unit
n_b	Background counts (under the region of the total absorption line)	-
n_n	Net counts in the total absorption line	-
p	Emission probability per decay for the considered photon energy, E	-
R	Radius of the distribution model	m
R_S	Radius of field of view	m
$u(x_i)$	Standard uncertainty of the input quantity x_i	The unit results from the input quantity.
$u_{rel}^2(x_i)$	Relative variance of the input quantity x_i	The unit results from the input quantity.
t	Measuring time	s
V	Distribution model	-
W	Angular correction factor	-
w	Calibration factor to calculate the activity per unit of surface area or mass of the radionuclide in question	m^{-2} or kg^{-1}
w_h	Calibration factor to calculate the radionuclide specific ambient dose equivalent rate	-
ζ	Mass per unit area	$kg \cdot m^{-2}$
z	Soil depth	m
z'	Variable of integration of the soil depth	-
ϑ	Polar angle	Degree
ε	Detector efficiency	
	a) per unit of surface area	m^2
	b) per unit of mass	kg
η_m	Cross section of the detector for photons from the polar segment, m	m^2
η_0	Intrinsic efficiency	m^2
ϑ_{ext}	External polar angle of the angular segment of interest	Degree
ϑ_{lim}	Limit angle of the distribution model	Degree
ϑ_{int}	Internal polar angle of the angular segment of interest	Degree
ϑ_{col}	Aperture angle of the collimated spectrometer	Degree
μ_{Air}	Linear attenuation coefficient of air	m^{-1}
μ_S/ρ_S	Mass attenuation coefficient of soil	$m^2 \cdot kg^{-1}$
$\rho_S(z)$	Soil density as function of soil depth, z	$kg \cdot m^{-3}$
Φ	Density of flux of unscattered photons of energy E for distribution model V at the detector location	$s^{-1} \cdot m^{-2}$
$\left(\frac{\Delta\Phi_m}{\Phi}\right)_{E,V}$	Portion of flux density of unscattered photons of energy E resulting from polar angle segment m for distribution model V at the detector location	-
β	Relaxation mass per unit area	$kg \cdot m^{-2}$

4 Principles

4.1 Measurement method

In situ gamma spectrometry is a direct, physical method for fast determination of activity per unit of surface area or per mass unit of gamma-emitting radionuclides present in or deposited on the soil surface.

In situ gamma spectrometry can be considered as a screening method that can supplement soil sampling with a subsequent gamma spectrometry in the laboratory, with the following advantages:

— no time-consuming sampling and no test sample preparation necessary for laboratory;

— short measuring time;

— immediate availability of results in the field;

— representativeness of the results for a fairly large area corresponding to the field-of-view of the detector.

During the measurement, the detector is positioned preferably with the end cap down on an assembly jig.

For quantitative analysis of the pulse height spectra, assumptions are made concerning the distribution of radionuclides in soil, as well as the specific physical properties of the soil and the air.

Generally, the distribution of the radionuclides in soil is not known. The following ideal models are used:

— homogeneous distribution for natural radionuclides;

— surface deposition on the soil top layer for fresh, dry deposition of fallout;

— exponential decreasing activity concentration with increasing depth in soil following a fallout surface deposition of activity and subsequent migration down into deeper soil layers.

NOTE For the description of the activity distribution in the soil, simple exponential models are mostly used.

According to the assumed distribution model, for homogeneously distributed radionuclides, the activity is given in activity per unit of mass, whereas for artificial radionuclides, which are deposited on the surface and afterwards have migrated into the soil, the results are reported in activity per unit area.

4.2 Uncertainties of the measurement method

Uncertainties of the measurement method are principally due to

— uncertainty of the distribution of the radionuclides on and in the soil,

— contribution from other sources (e.g. activity in the surrounding air, see Annex A).

The main influence quantities are listed in Annex B, with the numerical values given in reference.[14]

5 Equipment

5.1 Portable *in situ* spectrometry system

An *in situ* gamma spectrometer consists of five main components, as listed below:

— high purity germanium detector or scintillation detector;

— pulse processing electronics;

— data recording and evaluation system;

— fixture for mounting the detector (e.g. tripod);

— cooling and, if required, shielding.

A portable *in situ* spectrometry system is recommended. It consists of a portable cooling device and electronics [the latter being a compact multichannel analyser system (MCA) with integrated high voltage power supply and pulse processing unit. Today, pulse processing is preferably performed as digital pulse processing]. Data transfer can be performed through telecommunication, e.g. by cable, radio, or satellite. The spectral data are transferred via cable, WLAN, or radio communication to a PC and stored on a hard disk or digital storage media (e.g. memory sticks, memory cards).

Since, in general, there is no power supply during the measurements in the field, it is useful that the measurement equipment is equipped with internal batteries for a self-contained operation.

5.2 Detector System

5.2.1 General

The high purity germanium system (HPGe System) is described in ISO 18589-3 and IEC 61275. Depending on the measurement objectives, two different types of germanium crystals (n type, p type) can be used. They can be built with different shapes, crystal mountings, end cap, and end cap window materials. The detector characteristics also define the measurement range, both in terms of gamma energy and count rate. A summary of the specifications is given in Annex C.

However, it shall be stressed that detectors capable of measuring at very low energies (like n-type detectors or detectors with special end cap materials) are not very useful for *in situ* measurements. This is due to the fragility of the detector and the large uncertainties of the measured activities caused by the high absorption of gamma radiation in the air and in the ground.

NOTE 1 Although quantitative measurements of radionuclides at low photon energies are not possible with p-type HPGe detectors for in situ measurements, the use of n-type detectors or detectors with special end cap materials provides the ability to identify radionuclides whose energies are below 60 keV.

For general applications, such as the determination of the activity concentration of naturally occurring radioactive material (NORM) in ground or soil contamination by artificial radionuclides, it is recommended to use germanium detectors with a relative detection efficiency of 20 % to 50 % and an energy range above 50 keV.

NOTE 2 In case of emergency measurements with high dose rates above 20 µSv/h (high photon fluxes) smaller germanium detectors with relative detector efficiency less than 20% are preferable.

It is recommended to use detectors which have an isotropic response function, i.e. detectors, which have no or nearly no dependency on the direction of the incident photons. This is the case if the surface area of the detector (i.e. its cross section perpendicular to the direction of the incident photon) is independent of the incidence angle, i.e. if the diameter of the crystal is approximately the same as its length.

NOTE 3 For detectors with a strong directional dependency, it is preferable to use mathematical methods to simulate detector efficiency since this dependency is inherently taken into account. On the other hand, these detectors are advantageous in cases where a limited field-of-view is required.

Under certain conditions, scintillation detectors [NaI(Tl), $LaBr_3$] can be used especially if high precision is not required. In this case, no cooling is required but the nuclide threshold decision and detection limit are higher due to lower energy resolution.

5.2.2 Field-of-view

The field-of-view of the detector is the soil surface area, from which 90 % of the unscattered detected photons originate. This area depends on the characteristics of the detector, the measurement height, the gamma energy, and the distribution of the radionuclide of interest in soil. The field-of-view is always calculated for an infinite measurement area.

5.2.3 Special requirements

The detector system shall comply with the special requirements for *in situ* measurements according to IEC 61275. Specifically, the following topics shall be considered.

a) The system shall be humidity-proof and waterproof (splashing). This is especially true for all mechanical and electrical connections between the preamplifier and multichannel analyser.

b) The crystal shall be mounted in the detector end cap in such a way that the mechanical stress of detector transport does not result in any detector damage. This may mean that special transport containers shall be used.

c) The operating temperature for the detector shall be in the range of –20 °C to +50 °C. (Higher temperatures at the detector end cap may result in worse vacuum in the cap).

d) The capacity of the cooling system shall be sufficient for a complete operation time. In case of loss of cooling (e.g. if the Dewar vessel for liquid nitrogen runs empty), the detector recycling time as specified by the supplier shall be taken into account.

NOTE 1 If the detector is cooled by liquid nitrogen, transport activities result in higher nitrogen consumption.

NOTE 2 For standard applications, high-purity materials for detector mounting, end cap, and end cap window are not required.

5.3 Pulse processing electronics

5.3.1 Components

The pulse processing system consists of the following components:

— detector high voltage power supply;

— spectroscopy amplifier;

— analog-to-digital converter (ADC);

— multichannel analyser (MCA).

Latest versions of commercial electronic units use digital electronics to process the pulses. In this case, the spectroscopy amplifier and the ADC are substituted by a digital signal processor.

It is highly recommended to use integrated pulse processing units. In this case, all the individual electronic components are integrated into one box, which in turn is connected to the detector preamplifier and a personal computer (PC).

The connection to the PC can be done by a serial connection (cable), by USB (cable), by WLAN (wireless), or by other types of radio communication (wireless). The PC should be battery operated.

5.3.2 Special requirements

The pulse processing electronics shall fulfil the following special requirements for *in situ* measurements; if no digital signal processing is used, the system should be temperature stabilized. This can be done by a digital spectrum stabilizer. Digital signal processors normally are not temperature sensitive; hence, stabilization is not required.

NOTE Stabilization can be done using the gamma line of ^{40}K at 1 461 keV.

It is preferable to use battery-operated electronics. The minimum operation time of the batteries should be 4 hours. Switching between battery and mains operation should be possible.

5.3.3 Requirements for the evaluation program

Software programs for evaluation of spectra of an *in situ* spectrometer shall have additional functionalities compared to those typically used in laboratory applications. These additional functions can be achieved by special add-on programs or modules. The following basic functions shall be available:

— performing energy calibration and, if required, energy stabilization;

— automatic peak location and peak area quantification. There should be the possibility of manual interaction (defining peak regions, etc.). The peak area quantification includes calculation of the peak position, the peak FWHM, the peak net area, and the peak area uncertainty. Multiplet deconvolution shall be possible;

— radionuclide identification algorithm, using a radionuclide library, which can be edited by competent users. The radionuclide identification includes calculation of radionuclide activities, decision thresholds, and detection limits according to ISO 11929. The algorithm shall also perform interference corrections for interfering radionuclide lines. The activities, decision thresholds, and detection limits shall be calculated for any user specified reference date.

Additional functions may be useful, such as the following:

— determination of the angular correction factor, W, of the detector;

— modification of the detector height above ground;

— computation of the activity, in $Bq \cdot m^{-2}$, for each radionuclide exponential distribution in the soil, with the possibility of variation of the relaxation mass per unit area from at least 3 $kg \cdot m^{-2}$ to 150 $kg \cdot m^{-2}$;

— computation of the activity, in $Bq \cdot m^{-2}$, for each radionuclide deposited on the soil surface;

— computation of the activity, in $Bq \cdot kg^{-1}$, for radionuclide which are homogeneously distributed in the soil;

— computation of the ambient dose rate at a height of 1 m above ground. The software shall allow to edit the factor f_D or $f_{\bullet}^{H^*(10)}$ which is used to convert the area or mass specific activity into air kerma rate or ambient dose equivalent rate in air.

5.4 Assembly jig for a detector system

The detector mounting should be able to position the detector system at different heights. The assembly should be built from materials with a low atomic number and low density (aluminium, plastic material, wood). The assembly should have low intrinsic activity concentration. Usually, the detector is mounted at a height of 1 m.

Most mounting assemblies are constructed as tripods.

5.5 Collimated detector

5.5.1 Construction

An *in situ* gamma spectrometer equipped with a collimated detector is a special case of an *in situ* gamma spectrometer. The collimator reduces the field-of-view of the detector. The collimator defines the solid angle of detection which delineates a finite measurement area at the surface of soil. It allows filtering the flux of photons from outside this measurement area.

NOTE Typical fields of application of *in situ* gamma spectrometer with collimated detector are:

— activity measurement with a reduced field-of-view,

— activity measurement in case of external radiation influence (e.g. airborne activity),

— increase of the upper measurement limit (intensity of the radiation field, see B.10), and

— measurements inside the nuclear facilities.

In situ gamma spectrometer with a collimated detector consists of a portable detector with a cylindrical shape collimator (see Figure 1).

The design of the collimator depends on the objectives of the *in situ* measurement and on the local conditions (energy and intensity of external radiation fields that have to be attenuated). The collimator is characterized by the aperture angle and the mass per unit area.

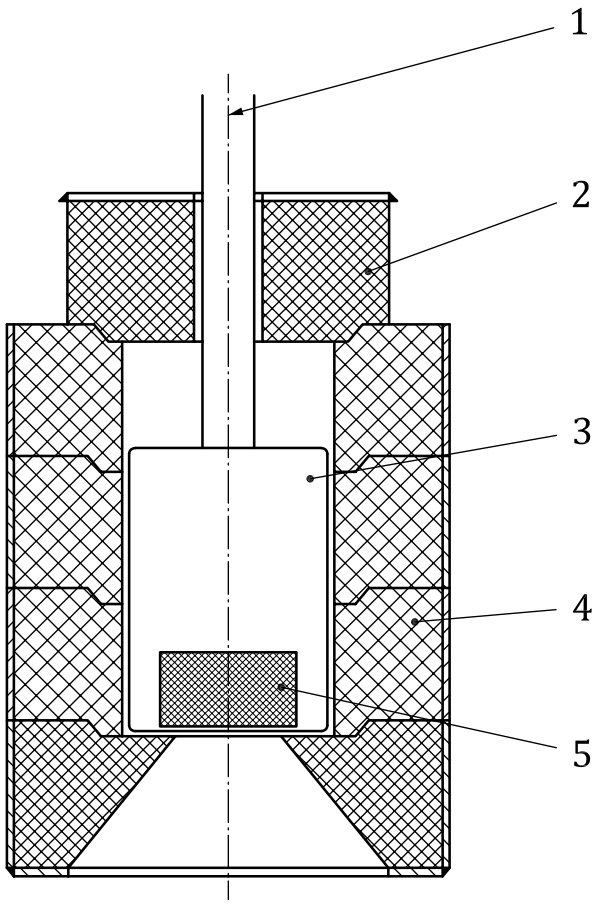

Key

1 axis of symmetry
2 rear shielding
3 detector
4 lateral shielding
5 detector crystal

Figure 1 — Diagram of arrangement of detector and cylindrically designed collimator

The wall thickness of the collimator is typically 25 mm to 60 mm when lead is used as the shielding material. The housing of the detector is enclosed by the collimator (typical distance 5 mm). A back shield may enhance the shielding effect.

The axis of symmetry of the detector and the axis of the collimator are identical. The position of the detector inside the collimator shall be adjusted reproducibly.

5.5.2 Collimator parameter

5.5.2.1 Aperture angle

The aperture angle ϑ_{col} is mainly dependent on collimator construction, dimensions and material, as well as on its position in relation to the detector.

The aperture angle is defined by the radius of the field-of-view of the collimated spectrometer for a photon energy of 662 keV, an extensive and infinite surface contamination and a detector height of 1 m above ground.

NOTE 1 The range of the aperture angle of a collimator is typically from 40° up to 70°. The aperture angle ϑ_{col} is calculated with the radius R_s of the field-of-view of the collimated detector (see Annex D).

$$\vartheta_{col} = arc\tan\left(\frac{Rs}{d}\right) \tag{1}$$

NOTE 2 The field-of-view of the collimated detector gives no reliable indication for the measurement area in case of higher photon energies. The aperture angle of the collimator is different from the aperture angle defined by the technical layout of the collimator.

5.5.2.2 Mass per unit area

The mass per unit area of a collimator, ζ_{col}, is given for a polar angle of 90°. It is important for shielding of the external radiation (radiation background).

NOTE The range of the mass per unit area is typically from 200 kg · m^{-2} up to 900 kg · m^{-2}.

5.5.2.3 Materials

For the construction of collimators, material of high density and high atomic number is used. Those materials are lead, tungsten (sintered), and copper. Materials used for the construction of collimators are shown in Table 2.

NOTE For photon energies above 100 keV, the influence of the density is stronger than that of the atomic number. High-density materials may reduce the mass of the collimator by reduced wall thickness at constant shielding effect.

For reduction of the radiation intensity in case of collimators constructed of lead or tungsten, a layer of copper or tin/copper-alloy inside the collimator is advantageous.

Table 2 — Materials suitable for collimator construction and their parameters

Material	Density kg · m^{-3}	Atomic number	Comments
Tungsten, sintered	approx. 1,8 · 10^4	74	Expensive, high shielding effect
Lead	1,13 · 10^4	82	Mostly used as shielding material, good value
Copper	0,90 · 10^4	29	Low self activity, low shielding effect, not suitable for high photon energies

6 Procedure

6.1 Calibration

Large area calibration standards are not commonly available for *in situ* spectrometry. Therefore, calibration procedures are developed that combine the characteristics of the detectors, the physical data describing the soil and the air, as well as assumptions of the distribution of the radionuclides in the soil.

Of paramount importance is the determination of a realistic model of the distribution of the radionuclides in the soil. Usually, mathematical models describe an exponentially decreasing activity with increasing depth.

The projected surface activity is described as

$$a(\zeta) = a_o \cdot \exp\left(-\frac{\zeta}{\beta}\right) \tag{2}$$

where ζ is defined as:

$$\zeta(z) = \int_0^z \rho_S(z') \cdot \mathrm{d}z' \tag{3}$$

Limiting cases are

$\beta \to \infty$ for a homogeneous distribution of radionuclides in soil, and

$\beta = 0$ for a perfect plane surface source.

β depends on the origin and the properties of the radionuclide, as well as the composition of the soil (chemical and physical properties of the soil, pH, cation exchange capacity, content of organic compounds, soil texture, etc.). Additionally, the nature of the deposition (dry or wet) and the time span since deposition shall be taken in account for determining the migration of the radionuclides through the soil.

NOTE 1 The distribution of the radionuclides in the soil is determined by laboratory analysis of samples of each soil layer collected along a vertical profile (see ISO 18589-1 and ISO 18589-2). Soil samples are collected at different depths down to the layer where the contribution of the radionuclide activity to measurement results is no longer significant (usually at a depth of approximately 25 cm, depending on photon energy). Samples of each layer are measured by gamma spectrometry in the laboratory following ISO 18589-3.

NOTE 2 The parameter “relaxation length” is only used in case of constant vertical density of soil.

The efficiency per mass or surface area shall be determined based on the photon energy, the distribution of the radionuclides in soil, the absorption properties of the soil and the air, as well as the detector system and its height above the ground.

The efficiency functions are determined either with a procedure that combines the results of the calibration measurements with the result of the model calculation or with a calibration procedure based exclusively on a numerical approach.

For both calibration methods, the detector efficiency shall not vary with the azimuth angle (angle of the horizontal plane).

6.2 Method of combined calibrations

NOTE See Reference [8].

6.2.1 General

The detector efficiency, ε, is calculated according to the following formula:

$$\varepsilon = \eta_0 \cdot G \cdot W \tag{4}$$

Figure 2 shows the links between specific empirical and model quantities and the calibration of an *in situ* gamma spectrometer.

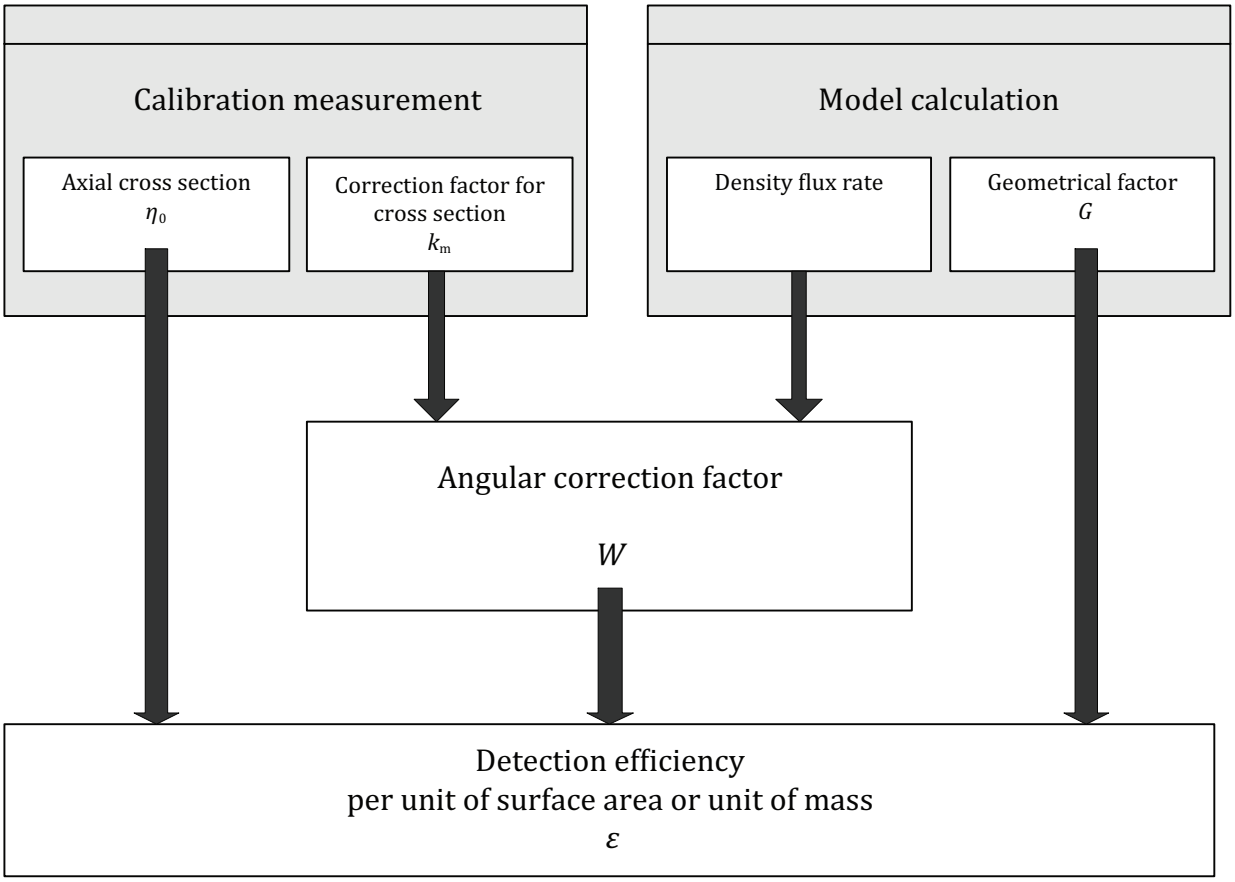

Figure 2 — Diagram of empirical and model quantities and their link to the calibration of an *in situ* gamma spectrometer

6.2.2 Intrinsic efficiency

The intrinsic efficiency, η_0, of a detector is determined by the measurement of a calibration point source. The standard calibration source is positioned at a defined distance from the geometrical centre of the detector crystal in direction of the axis of symmetry of the crystal. The net count rate for full energy peaks from the calibration source are recorded. The gamma energies of the source should be in the range of 0,060 to 2 MeV; the distance from the detector should not be less than 0,5 m.

By preference, multiline sources like ^{133}Ba in combination with ^{152}Eu or mixed gamma radionuclide calibration standards are used to calibrate detector efficiency.

The intrinsic efficiency, η_0, is defined according the following formula:

$$\eta_0 = \frac{\left(n_g - n_b\right)/t}{\Phi} = 4\pi \cdot d^2 \cdot \frac{\left(n_g - n_b\right)/t}{a_K \cdot p} \tag{5}$$

Usually, a function is generated from the individual values of η_0, which is determined from discrete photon energies. This function, $\eta_0(E)$, describes the dependency of the intrinsic efficiency as a function of the photon energy. Using this function, the intrinsic efficiency can be computed for all photon energies in the calibration range.

6.2.3 Geometry factor

The geometry factor, G, depends on photon energy, E, and is calculated on the basis of the model assumptions on the distribution of the radionuclides in or on the soil, the detector height, the attenuation coefficient of the air, and the mass attenuation coefficient of the soil.

The horizontal and vertical distribution of the radionuclides in the soil influence the geometry factor and the computed results; therefore, a realistic assumption of the distribution is essential.

According to 3.1.9, the field-of-view of a spectrometer is defined as the area, centred on the detector, from which 90 % of detected unscattered photons originate. This surface corresponds to 90 % of an infinite measurement area. If the measurement area is larger than the field-of-view, it is acceptable to apply the model of an "area of infinite extent" to calculate the geometry factor. This leads to an underestimation of the activity per unit area of ground or surface less than 10 % due to the difference between the model and the actual area measured.

The formulae for calculating the geometry factors (geometry functions) for distribution models with finite and infinite plane surfaces are given in E.1 and E.2. Important geometry functions for the detector height of 1 m are shown graphically in E.3 and E.4.

If the measured surface is smaller than the detector's field-of-view, infinite plane surface distribution models cannot be used. In these cases, the geometry factor shall be calculated based on the actual geometry of the area to be measured. As an approximation, geometry factors can be calculated for measurement surfaces with finite planes using the geometry functions given in E.2. In this case, the radius of the distribution model shall be selected so that its surface area is more or less the same size as the measurement area. The formulae and an example for circular measurement surfaces are given in E.2. An example for calculating a geometry factor for a finite plane surface distribution is given in E.5.

6.2.4 Angular correction factor

The angular correction factor, W, takes into account that a part of the photons do not enter the crystal along the detector symmetry axis, but with side angle, which depends on the size of the field-of-view. This angular dependence of detector efficiency should be considered.

The angular correction factor depends on the detector type, the photon energy, and the angular distribution of the incoming photon without scattering at the detector location. The computation of the angular correction factor is complex. The calculation can be omitted if the detector has no or only a small dependency on the polar angle, ϑ. In this case, the value of the angular correction factor is approximately 1 for all photon energies and all distribution models.

In general, this is applicable for photon energies larger than 100 keV, if the ratio between the diameter and the length of the crystal of the detector used is 1 ± 0,1.

The determination of the angular correction factor is always necessary if the energy of photon absorption line is less than 100 keV or if the diameter of the detector crystal deviates by more than 10 % from its length. The solution of the integral is difficult to obtain and, therefore, the integration is replaced by a summation. The polar angle, ϑ, is divided in M subsegments. One subsegment should not be larger than 10°. When using a collimated detector, it should not be more than 5°. For every subsegment, the

portion of unscattered photons, $\Delta\Phi_m / \Phi$, is calculated and multiplied by the corresponding correction factor for the angular coefficient, k_m. The correction factor, W, is the sum of these products:

$$W = \sum_{m=1}^{M} k_m \cdot \left(\frac{\Delta \Phi_m}{\Phi} \right) \tag{6}$$

Angular coefficients, k_m, are determined by calibration measurements with point source activity standards. In a first step, for every polar angular segment m, the surface efficiency, η_m, for unscattered photons is determined. The angular coefficient, k_m, is given by

$$k_m = \frac{\eta_m}{\eta_0} \tag{7}$$

Formulae to calculate flux density rates $\Delta\Phi_m / \Phi$ for frequently used model geometries are shown in E.6 and E.7.

Calculation examples to determine angular correction factors are shown in E.8 and E.9.

NOTE 1 Usually, discrete correction factors, k_m, are determined using multiline or mixed radionuclide sources for every polar angular segment, m. These are parameterized in two steps, in a way that every polar angular segment, m, results in a correction factor $k(E)_m$ as function of the photon energy, E. This gives an indication of the variation of surface efficiencies for a wide range of photon energies.

NOTE 2 When using a collimated detector system, the absorption of the collimator can be interpreted as angular dependence of the detector efficiency. Therefore, correction factors or correction functions for surface efficiencies are always determined for the detector system (detector and collimator).

6.2.5 Numerical calibration procedure

6.2.5.1 General

No source is needed when using the numerical calibration procedure.

NOTE This does not exclude when one or more sources are used for the characterization of the detector.

Basic principles and the individual mathematical steps are described in Figure 3 below.

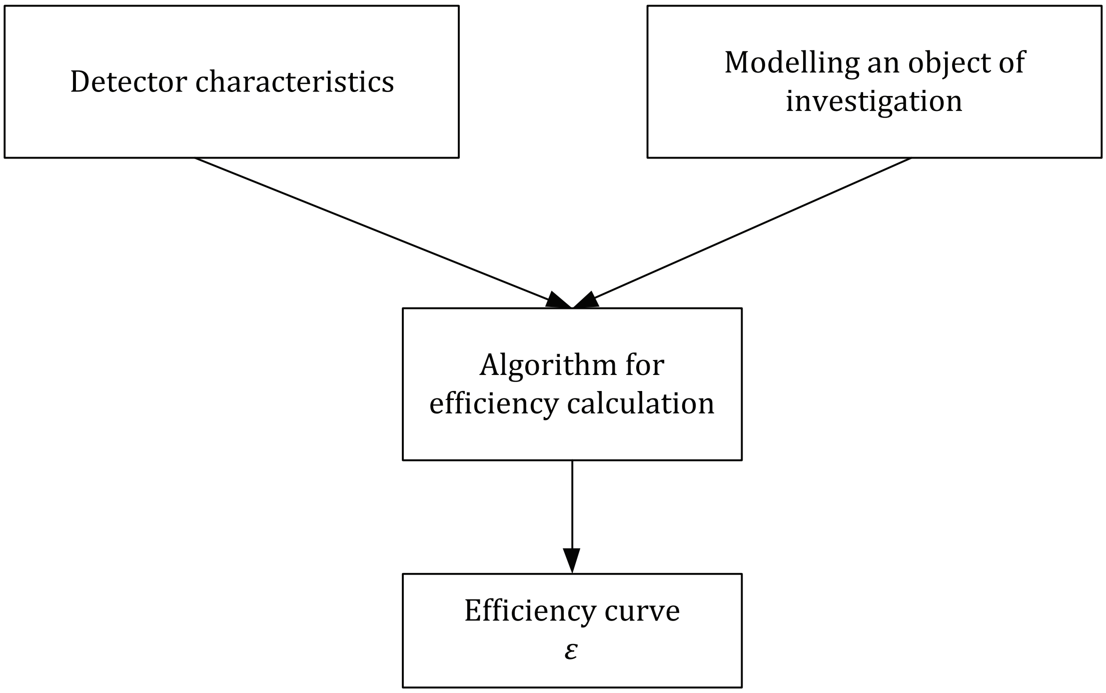

Figure 3 — Schematic diagram of the individual components for a numeric calibration

Numerical calibrations are based on three components: detector characteristics, model of the measuring object, and algorithm for efficiency calculation.

6.2.5.2 Detector characteristics

The detector characterization is given by a mathematical expression that describes the efficiency of the detector for point sources as a function of the gamma energy, of the distance from the detector crystal, and the solid angle.

The mathematical expression is determined using Monte-Carlo simulations on one hand, and by adjusting the parameters of the simulation in such a way that the simulation is fitted to real measurements of point and area sources on the other hand.

In this case, sources are necessary. This characterization procedure can be carried out by the manufacturer, in order that the user does not have to perform time-consuming calibration measurements.

Sources used to generate the detector characteristics shall be accurate and certified.

6.2.5.3 Modelling the measuring object

Modelling the measuring object means the mathematical description of the measurement geometry. Depending on the software used, more or less complex descriptions are possible.

A distinction is generally made between surface distribution for fresh deposits on the soil surface, the uniform distribution for homogeneous dispersal to a depth of 40 cm below the soil surface (natural radionuclides for example), and the distribution according to exponential decay with depth in soil for older deposits.

NOTE Several other models can be used for the depth distribution, e.g. Lorentz slab, multi-slab, bi-exponential and other distribution models.

Usually, the description only concerns the linear dimension of the measured surface area (diameter, radius), the height of the detector above the surface area (usually 1 m), the soil density, as well as the

penetration depth of the contamination (relaxation mass density). In many cases, the true values for this quantity are not known.

A distinction has to be made between the distribution of artificial and natural radionuclides. In general, artificial radionuclide deposition on soil from fallout yields over time has an exponential distribution in the soil, whereas the natural radionuclides have a homogeneous distribution.

6.2.5.4 Algorithm for efficiency calculation

By combining the information according to 6.2.2 and 6.2.3, the efficiency curve is calculated for the measurement object. Based on the consideration in 6.2.4, two types of efficiency curves are required:

ε_F to describe the efficiency per unit of surface area, and

ε_V to describe the efficiency per unit of mass (for homogeneous distribution).

7 Quality assurance and quality control program

7.1 General

Quality control operations should meet the requirements of ISO/IEC 17025. The influencing variables affecting each measurement method are discussed in the corresponding relevant ISO/IEC standards.

7.2 Influencing variables

Some variables may have varying degrees of influence on the measurement. Special care shall be taken in order to limit as much as possible the influence of parameters that may bias the measurement and lead to a result non-representative of the situation under investigation. Failure to take sufficient precautions requires corrective factors to be applied to the measurement result.

The influencing variables affecting this measurement method are discussed in Annex B.

7.3 Instrument verification

Major instrument parameters (efficiency, background) should be periodically checked within a quality assurance programme established by the laboratory and in accordance with the manufacturer's instructions.

7.4 Method verification

A verification of method accuracy shall be run periodically. This may be accomplished by

— participating in national or international intercomparison exercises,

— analysing reference materials.

7.5 Quality control program

7.5.1 General

For every measuring system, a quality assurance plan has to be established, describing the program and actions to ensure a constant quality of measurements with an *in situ* gamma spectrometer.

The quality assurance plan includes, among others,

— periodical quality checks,

— verification/test measurements,

— special qualification and training, and

— documentation of quality controls.

7.5.2 Description of periodical quality checks

7.5.2.1 Functional test

At the beginning of every measuring campaign, after the cooling of the detector, the system has to be checked regularly for a correct function and reproducibility of results. The measuring system has to be placed in the measuring position. The spectrum is recorded and analysed. The position of the energy line of the natural radionuclides (i.e. ^{40}K, ^{214}Bi, ^{226}Ra, ^{214}Pb) and peak shapes are analysed and stabilized or recalibrated if necessary.

7.5.2.2 Testing detector efficiency and peak width

At least once a year, the detector is submitted to a periodic check. In case of frequent warm-up cycles, a check in shorter periods is necessary. The detector is checked with a source of known activity (e.g. ^{152}Eu) at reproducible conditions. Radionuclides of the standard source should cover a wide range of gamma energies; there should be at least three gamma lines at low, at medium, and at high energy. The constancy of the detector efficiency and peak width are determined for at least three energies. Results are compared with previously performed inspections. Significant differences lead to additional checks and appropriate actions.

7.5.2.3 Test of background

At least once a year or after suspicion of a contamination, the background has to be controlled by comparing the latest background spectrum with previous ones.

7.5.3 Measurement verification

For quality assurance purposes, periodic participation in verification measurements is recommended. These verification measurements are organized by offices observing environmental radioactivity. To verify detector efficiency, the activity of a point source, placed in a reproducible distance, is determined.

All participants perform and analyse measurements on a selected area with a nominal known activity per unit of surface area and/or mass (i.e. by evaluating samples, or known sources). The *in situ* results of the participating teams are compared to the nominal values and to the mean values calculated by the other teams.

7.5.4 Qualification

It is necessary to determine a training plan for a periodical qualification of the measuring personnel, who is entrusted with the planning of the measurement, the measurement itself, data analysis, and the report drafting.

It is recommended to educate the competent staff by courses about *in situ* measurement technique organized by experts, educational establishments, or measurement equipment manufacturers and software producers and to train the staff by periodical measurement campaigns or training programs.

7.5.5 Documentation of quality controls

Every institution has to keep records on dates of performance tests and their results. Reports should allow the detection of aberrations and their adjustment retrospectively.

7.6 Standard operating procedure

A standard operating procedure contains instructions about

— planning of the measurement,

— measurement procedure,

— practical application of measurement,

— analysis, and

— reporting.

8 Expression of results

8.1 Calculation of activity per unit of surface area or unit of mass

The activity, a, per surface area or per mass of a radionuclide is determined according to the following formula:

$$a = \frac{\left(n_g - n_b\right)/t}{p \cdot \varepsilon} = w \cdot \left(n_g - n_b\right)/t \tag{8}$$

The decay of a radionuclide during the measuring time is not considered in Formula (8) above. For measurement of short-lived radionuclides, a correction factor is required.

According to the assumed distribution model, for homogeneously distributed radionuclides, the activity is given in activity units per mass, whereas for artificial radionuclides, which are deposited on the surface and afterwards have migrated into the soil, the results are reported in activity units per surface area.

In soils that have been ploughed to a depth of over 0,25 m, such as in farmland, the activity per unit of mass of deposited radionuclides has to be analysed by assuming uniform distribution.

In a second step, the conversion into activity per unit of surface area is possible considering the plough depth and the density of the soil.

During analysis of radionuclides, the daughters of the decay chains have to be considered.

NOTE Deviating results in activity of energetically different lines of the same radionuclide could indicate an incorrect model assumption.

8.2 Calculation of the characteristic limits and the best estimate of the measurand as well as its standard uncertainty

8.2.1 General

The parameters of ionizing radiation measurements (decision threshold, detection limit, and the limits of the confidence interval) are named as characteristic limits. The best estimate of the measurand and its standard uncertainty are calculated from the primary result and their standard uncertainty (see ISO 11929). In the case under consideration, the measuring value, a, is the primary result.

The activity per unit of surface area or mass, a, of any detected radionuclide and for a given distribution model, V, is determined from the net count rate of an undisturbed energy line with the photon energy, E [see Formula (8)].

NOTE The following calculation does not take into account any correction of the energy lines due to interferences. Also, no covariances are considered nor are radionuclide specific activities from several energy lines calculated.

8.2.2 Standard uncertainty

According to ISO 11929, all multiplicative parameters considered in the analysis of the model are summarized in the calibration factor, *w*.

Where

$$w = \frac{1}{\varepsilon \cdot p} = \left(p \cdot \eta_0 \cdot G \cdot W\right)^{-1} \tag{9}$$

The relative variance of *w* is calculated from the quadratic addition of the relative single variances, where the uncertainty of the emission probability and the decay correction can be neglected.

$$u_{rel}^2(w) = u_{rel}^2(\eta_0) + u_{rel}^2(G) + u_{rel}^2(W) \tag{10}$$

The standard uncertainty $u(a)$ of a is as follows:

$$u(a) = \sqrt{w^2/t^2 \cdot \left[u^2(n_g) + u^2(n_b)\right] + a^2 \cdot u_{rel}^2(w)} \tag{11}$$

8.2.3 Decision threshold and detection limit

The determination of the decision threshold and the detection limit is primarily regularized in ISO 11929. For the used analysis model in *in situ* gamma spectrometry, the following apply:

Decision threshold:

$$a^* = k \cdot \sqrt{c_0} \tag{12}$$

Detection limit:

$$a^{\#} = \frac{2 \cdot a^* + k^2 \cdot c_1}{1 - k^2 \cdot c_2} \tag{13}$$

With the coefficients

$$c_0 = \frac{n_b + u^2(n_b)}{t^2} \cdot w^2 \,, \tag{14}$$

$$c_1 = w / t \,, \tag{15}$$

$$c_2 = u_{rel}^2(w) \,, \tag{16}$$

and

$k_{1-\alpha} = k_{1-\beta} = k$

NOTE 1 Formulae (13) and (16) directly result in the important relation that the detection limit can only be given if $k \cdot u_{rel}(w) < 1$.

NOTE 2 Mostly, *k* is selected as 1,645.

A calculation example of decision threshold and detection limit activity is shown in F.4.

8.2.4 Limits of confidence interval and best estimate of the measurand

The lower limit $a^{\triangleleft}$ and the upper limit $a^{\triangleright}$ results from the equation

$$a^{\triangleleft} = a - k_p \cdot u(a)$$

where $p = \omega \cdot (1 - \gamma / 2)$ and $a^{\triangleright} = a + k_q \cdot u(a)$

where

$$q = (1 - \omega \cdot \gamma / 2)$$

in ISO 11929.

If

$$a^{\triangleleft\triangleright} = a \pm k_{1-\gamma/2} \cdot u(a)\,, \tag{17}$$

Formula (17) holds.

NOTE 1 Mostly, $k_{1-\gamma/2}$ is selected as 1,96 ($\gamma = 0{,}05$).

An example for calculating the confidence limits is shown in F.5.

The primary measurement result, a, can be considered as best estimate, $\hat{a}$, under the condition $a \geq 4 \cdot u(a)$. In this case, the following approximation applies: $\hat{a} = a$ and $u(\hat{a}) = u(a)$.

NOTE 2 For a <4 $u(a)$, the best estimate and its standard uncertainty are computed according to ISO 11929, because both quantities differ significantly from the primary measurement result and its standard uncertainty. In practice, one is often in the region of the decision threshold.

8.3 Calculation of the radionuclide specific ambient dose rate

The ambient dose rate of a single radionuclide can be determined from the results of the activity per unit of surface area or mass. This is of interest if it is necessary to determine the individual parts of the artificial and the natural gamma radiation separately.

The amount of the kerma dose rate $\dot{D}_{V,N}$ or the ambient dose equivalent rate $\dot{H}^*(10)_{V,N}$ for every single radionuclide for the distribution model, V, and radionuclide, N, as a product of the activity per unit of surface area or mass, a, and the factor f_D or $f_{\dot{H}^*(10)}$ conversion factor for the activity per unit of surface area or mass, are calculated as follows:

$$\dot{D}_{V,N} = f_D \cdot \frac{(n_g - n_b)/t}{p \cdot \varepsilon} = f_D \cdot a \tag{18}$$

or

$$\dot{H}^*(10)_{V,N} = f_{\dot{H}^*(10)} \cdot a \tag{19}$$

In this case, depending on the calculation model, the relative variance, w_h, resulting from the addition of the quadrates of the relative single variances, has to be verified by analogy Formula (10). To determine

the correct uncertainties, the geometry factor and the dose rate factor have to be considered separately or together. In this case, they are calculated as follows:

$$u_{rel}^2(w_h) = u_{rel}^2(\eta_0) + u_{rel}^2(G \cdot f_D) + u_{rel}^2(W) \tag{20}$$

or

$$u_{rel}^2(w_h) = u_{rel}^2(\eta_0) + u_{rel}^2(G \cdot f_{\dot{H}^*(10)}) + u_{rel}^2(W) \tag{21}$$

The factor f_D or $f_{\dot{H}^*(10)}$ depends on the radionuclide, its distribution in the soil, and the height of the detector. The calculation is carried out by e.g. Monte-Carlo method. Values of the conversion factor f_D or $f_{\dot{H}^*(10)}$ for calculation of the radionuclide specific ambient dose rate as kerma rate at 1 m height above the ground for different radionuclides and relaxation masses per unit area, β, are listed in Annex G.

NOTE 1 Values for conversion factor, f_D, for homogeneous distribution in soil of the natural radionuclides of the Uranium-Radium decay chain, the Thorium decay chain, and for ^{40}K are taken from the table in G.1.

Thereby, radioactive equilibrium of the radionuclides within both decay chains is assumed. Values of the conversion factor f_D or $f_{\dot{H}^*(10)}$ for some relevant artificial radionuclides and various relaxation masses per unit area, β, are listed in G.2 and G.3. In case of ^{137}Cs, the factor of the daughter nuclide ^{137m}Ba is used to calculate the kerma rate.

NOTE 2 The EURATOM guidelines claim the reporting of the ambient dose rate as ambient dose equivalent rate $\dot{H}^*(10)$. At the time of publication, conversion factors are published for a limited number of radionuclides.[9,10]

An example for dose rate calculations is shown in G.4. The total dose rate results from the summation of the individual contributions of the considered radionuclides.

NOTE 3 Principally, the validity of the distribution model can be verified by a comparison between the value of dose rates determined by *in situ* gamma spectrometry and the value measured with an integrating meter (e.g. ionizing chamber or scintillation dosimeter) as far as the amount of cosmic radiation is considered. However, in practice, due to the measurement uncertainty of both procedures — especially at small contaminations — comparisons can hardly be made.

9 Test report

The test report has to fulfil the requirements of ISO/IEC 17025 and contain at least the following information:

a) a reference to this part of ISO 18589 (i.e. ISO 18589-7);

b) data for all relevant information, which may have influence on the result: used radionuclide library, analysis parameters, topographical or meteorological circumstances, etc.;

c) labelling of the measured area, if applicable geographic coordinates;

d) name of the radionuclide, radionuclide specific activity per unit of mass or surface with the associated *k*-values and its decision threshold, detection limit or activity with confidence intervals, the unit, and the distribution model used for activity calculation [soil composition for $G(E, V) < 100$ keV (see Annex H)];

e) the result of measurement, in accordance with ISO 11929;

f) optionally, radionuclide specific values of the ambient dose equivalent rate.

Annex A
(informative)

Influence of radionuclides in air on the result of surface or mass activity measured by *in situ* gamma spectrometry

The graph in Figure A.1 shows the expected overestimation of the specific activity due to an activity concentration of radionuclides in air of 1 Bq · m^{-3} as a function of photon energy. The specific activity calculated is based on a distribution model with infinite homogeneous activity distribution and a detector height of 1 m above ground. The anisotropy of the detector efficiency is not considered. It should be stressed that most of the gammas seen in the detector come from the air around and above the detector. In such a situation, it would be advisable to use a collimator which limits the field-of-view of the detector to the volume between detector and ground.

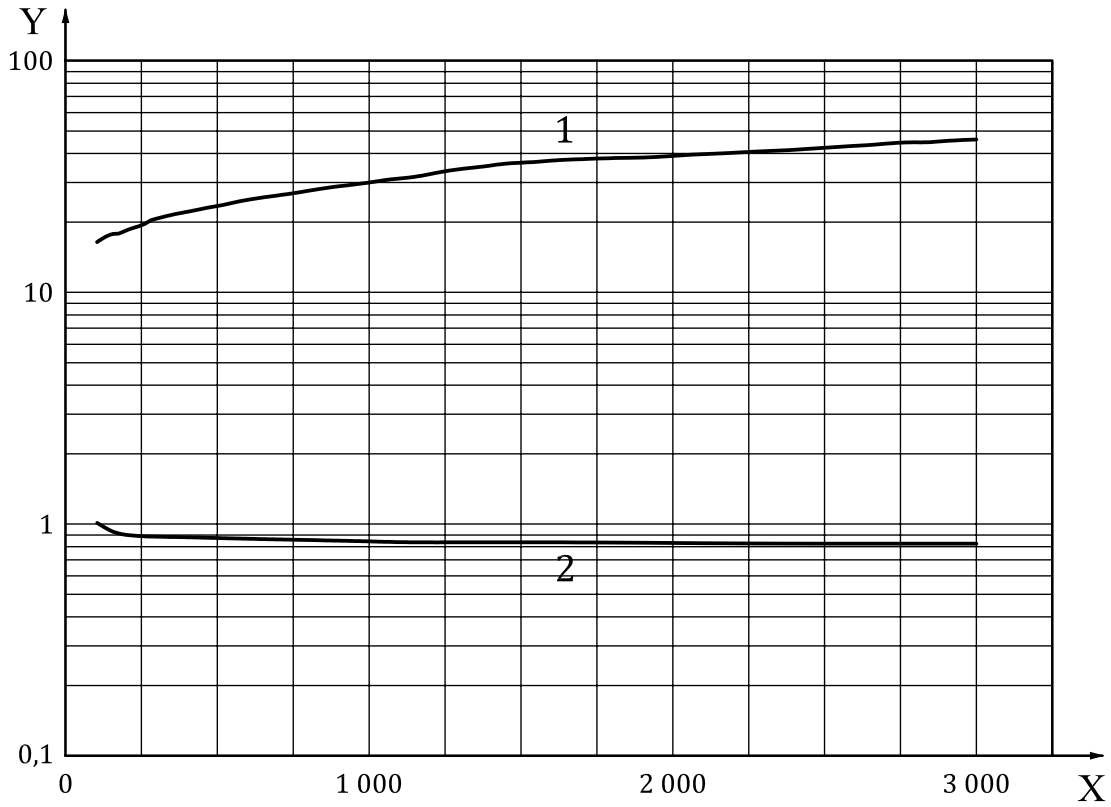

Key

1 deposit on the ground surface

2 uniform distribution

X *E* in keV

Y in Bq · kg^{-1} or in Bq · m^{-2}

Figure A.1 — Activity per unit of surface area in case of deposition on the surface or activity per unit of mass in case of homogeneous distribution in the soil, caused by activity in the air with an activity concentration of 1 Bq · m^{-3}

Annex B
(informative)

Influence quantities

NOTE Most of the parameters listed below are quantified in Reference.[14]

B.1 Measurement location requirements

The measurement locations should be:

— flat surfaces (fields, pasture lands, or lawns) without any obstacles (trees, rocks, buildings),

— as large as possible (larger than the detector's field-of-view, see Annex D),

— untreated (although ploughed fields can be used to determine natural radionuclides), and

— without any non-uniform part of the subsurface (rocky outcrops or underground structures).

NOTE 1 After deposition of radionuclides by rain, measurements in areas in which rain water covers the ground (dips) can produce wrong results.

NOTE 2 Larger elevations (ridges, banks, hills) near the measurement location (also outside the field-of-view of the detector) may disturb the results.

NOTE 3 In case of a sloping surface, the contamination deposits following rainfall are not homogeneous: It may be lower on the slopes and higher in the hollows where it tends to accumulate.

Care shall be taken to maintain the detector's axis of symmetry perpendicular to the ground surface.

B.2 Roughness of the ground surface

Roughness of the ground surface may affect the detector's field-of-view in that certain irregularities of the terrain may hide areas located behind them. This effect may be particularly pronounced where there is a relaxation mass with a low surface density. In this case, a value of 3 $kg \cdot m^{-2}$, and not the value zero (which is used for perfect surface deposits), should be used for the relaxation mass per unit area.

NOTE In reality, a perfectly flat surface source is not found; there is always some attenuation due to vegetation, ground roughness or a slight penetration of the activity into the soil. However, the value β=0 can be used to calculate the equivalent surface deposition, i.e. a plane surface deposition that would produce the same full-energy peak count rate in the detector as the actual deposition and source geometry. The equivalent surface deposition is always an underestimate of the true deposition.

B.3 Plant ground cover

Dense, moist plant cover may attenuate gamma radiation, which would result in the activity being underestimated. A radioactive deposition on plant ground cover would result in a modification of the measurement geometry.

B.4 Heterogeneities in soil contamination

Heterogeneities in the distribution of radionuclides modify the measurement geometry. They have a more or less significant effect depending on their magnitude, size and position in relation to the detector. The influence of areas close to the detector is larger and decreases with increasing distance. A quantitative

analysis of the acquired spectra is no longer possible if there is no information about the distribution of the radionuclides in or on the ground or if the distribution cannot be described by a realistic model.

For measurements during or shortly after rain fall, a quantitative analysis cannot be performed for the ^{222}Rn daughters ^{214}Bi and ^{214}Pb, as no exact distribution model can be given. Determination of the mass specific activity of ^{226}Ra shall be done in this situation by direct measurement or after decay of the deposited nuclides ^{214}Bi and ^{214}Pb. This can only be done after several hours.

B.5 Distribution of radionuclides in soil

The choice of the proper relaxation mass per unit area, β, has a strong effect on the result of the activity per unit of surface area. To estimate these influence parameters, the geometry functions $G(E,V)$, shown in E.3, can be used.

B.6 Soil composition

The determination of the surface or mass activity is based on assumptions related to soil composition and soil water content (Annex H). Any differences between the actual conditions and these assumptions can induce a large deviation, particularly in case of low photon energies (E < 100 keV) and high surface densities or relaxation masses (β > 30 kg · m^{-2}).

B.7 External contributions

Contributions from sources other than the soil (radioactive objects in the field-of-view or atmospheric contamination) can result in overestimation of the surface or mass activity.

A quantitative analysis of the spectra of an *in situ* spectrometer cannot be performed if there is significant influence of objects which do not belong to the measurement area (significant means that the signal produced by these objects is greater than the uncertainty of the signal produced by the field to be measured). This may happen if there is significant air activity. The influence of external contributions can be reduced by use of collimators.

NOTE These air contributions may result in a significant overestimation of the mass or surface activity. Annex A gives an example of an overestimation of the measured surface or mass activity for an activity concentration in air in Bq · m^{-3} as a function of photon energy. For example, for ^{131}I, an activity concentration of 1 Bq · m^{-3} is equivalent to the measurement of a surface activity of 20 Bq · m^{-2} (β = 0 kg · m^{-2}).

B.8 Off-ground height of the detector

For an active surface greater than the field-of-view:

— For a detector placed at 1 m above the ground surface, variation of height up to several centimetres has no significant effect on the measurement result.

For an active surface which is significantly smaller than the field-of-view:

— The position of the detector shall be measured with an uncertainty less than 5 % and shall be positioned at the centre of the active surface.

B.9 Calibration

Uncertainties resulting from the measurement of the detector efficiency and the angular correction coefficients contribute significantly to the overall measurement uncertainty. It is advisable to reduce them by accurate positioning of the calibration sources and by sufficiently long measurement times.

B.10 Influence of dose rate on measuring equipment

In case of very high surface or mass activities in soil, resulting in high flux densities, *in situ* gamma spectrometry would be of limited use due to the effects of dead times. However, a collimator could be used.

The energy deposited in the crystal of the detector per unit of time, a quantity that is proportional to the ambient dose rate, may be considered as a limiting parameter. It shall be possible to take quantitative measurements up to a dose rate of approximately 10 $\mu Sv \cdot h^{-1}$, which roughly corresponds to a measured surface activity of:

for deposits on the ground surface ($\beta = 0\ kg \cdot m^{-2}$): 4 $MBq \cdot m^{-2}$ of ^{137}Cs

1 $MBq \cdot m^{-2}$ of ^{60}Co

in case of uniform distribution in soil: 150 $kBq \cdot kg^{-1}$ of ^{40}K

in case of uniform distribution in soil and equilibrium with all the decay daughters:

15 $kBq \cdot kg^{-1}$ of ^{238}U

9 $kBq \cdot kg^{-1}$ of ^{232}Th

The spectrometer can be used at higher values by using an electronic system designed to work with high count rates or a collimator.

Collimators limit the field-of-view of the detector but require the efficiency correction factors to be specifically defined.

In the case of an active surface greater than the field-of-view, increasing the height of the detector does not result in any significant reduction of the count rate.

Annex C
(informative)

Characteristics of germanium detectors

C.1 Characteristics of germanium detectors

Table C.1 — Characteristics of germanium detectors for the *in situ* gamma spectrometry

Type of crystal	End cap material	Window material	Range of energy	Relative detection efficiency	Notes
p-Type coaxial	Al, Cu	same as end cap	50 keV – 10 MeV	20 – 100 %	1
p-Type broad energy p-Type planar	Al	Carbon epoxy, Be	10 keV – 3 MeV	20 – 50 %	2, 3, 4
n-Type coaxial	Al, Cu	Carbon epoxy, Be	10 keV – 3 MeV	20 – 100 %	1, 2, 3
n-Type planar	Al	Carbon epoxy, Be	10 keV – 3 MeV	20 – 50 %	2, 3, 4

The terms “broad energy” and “planar” are used by different suppliers, partly synonymously, partly for differentiation.

NOTE 1 Very large detectors are disadvantageous, as higher activities result in large dead times of the measurement system, which may make measurement impossible.

NOTE 2 Window materials made of Carbon epoxy are more stable than Be windows. Using detectors with Be windows requires much more careful handling.

NOTE 3 Extending the energy range to lower energies does not generate additional quantitative information, as the absorption of low energy photons in soil results in larger counting uncertainties.

NOTE 4 Some of the crystal types listed here have a strong direction dependency in the response function. This anisotropy therefore needs to be corrected. On the other hand, this may be advantageous, as side effects like air contaminations have relatively low influence on the measurement. In this case, one can avoid using collimators.

C.2 Photon transmissions for different types of detectors, windows, and end cap materials as a function of the photon energy

Figure C.1 shows the transmission of photons graphically, in percent, for different types of detectors, windows, and end cap materials as a function of the photon energy.[4],[5],[6]

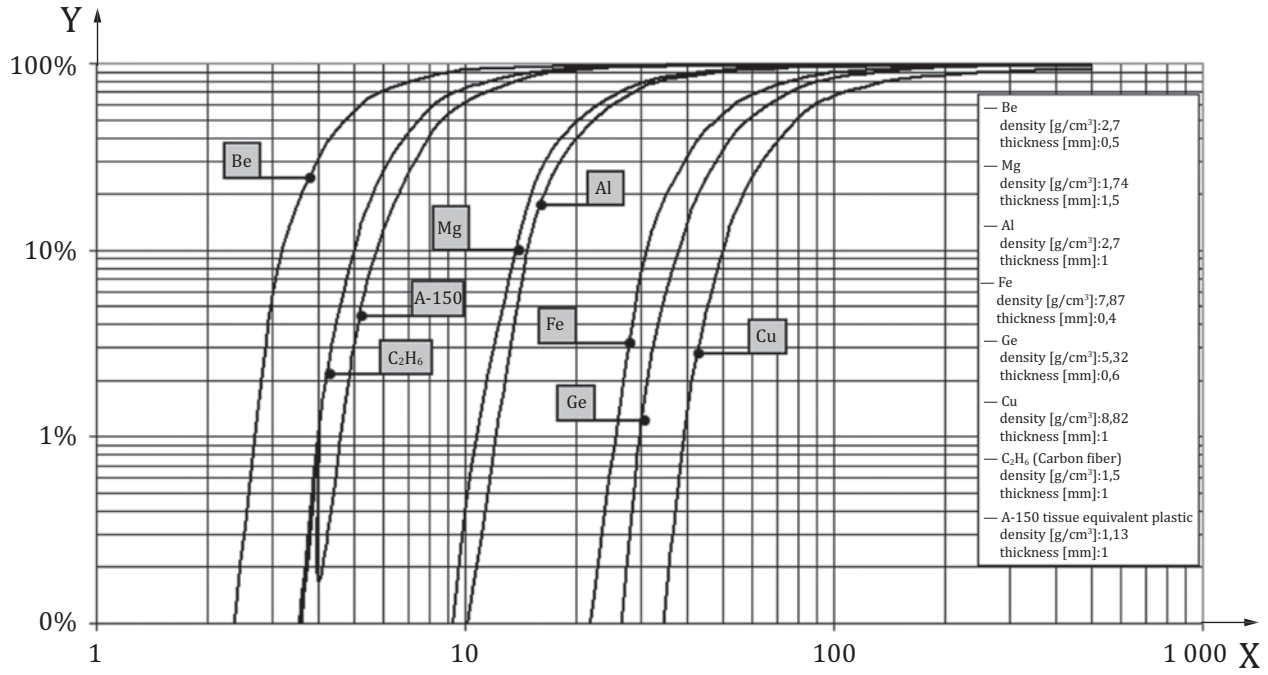

Key

X *E* in keV

Y transmission of photons

Figure C.1 — Transmission of photons for different types of detectors, windows, and end cap materials as a function of the photon energy[12]

Annex D
(informative)

Field-of-view of an *in situ* gamma spectrometer as a function of the photon energy for different radionuclide distributions in soil

D.1 Field-of-view of an *in situ* gamma spectrometer as a function of the photon energy for different radionuclide distributions in soil

In Figure D.1, the field-of-view of an *in situ* gamma spectrometer is shown as a function of the photon energy for different radionuclide distributions in soil and a detector height of 1 m. The mass attenuation coefficients of soil and the mass attenuation coefficient of air are taken from Annex H.

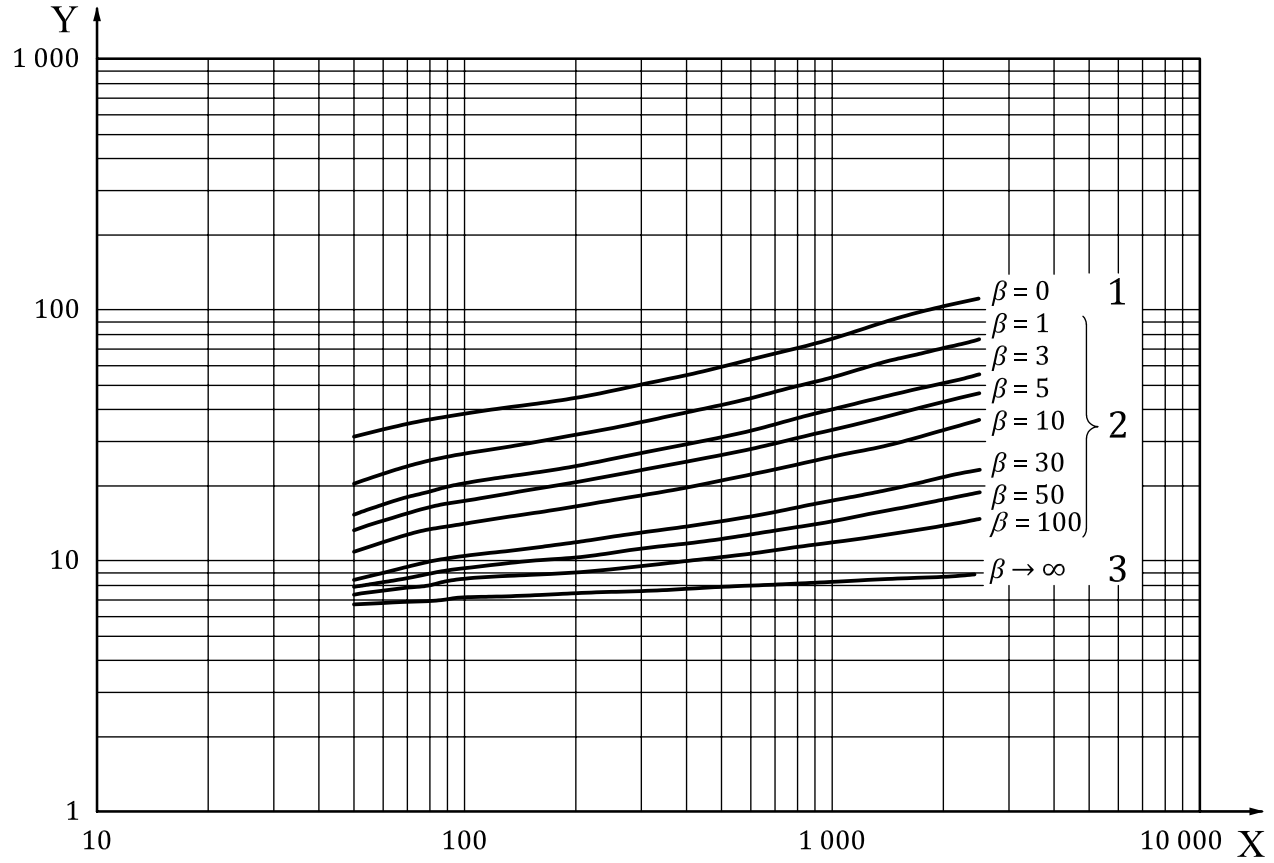

Key

1 deposit on the ground surface
2 exponential distribution
3 uniform distribution
X E in keV
Y R_S in m

Figure D.1 — Field-of-view of an *in situ* gamma spectrometer is shown as a function of the photon energy for different radionuclide distributions in soil and a detector height of 1 m, with relaxation mass per unit area, β, in kg·m^{-2} as parameter

D.2 Field-of-view of an *in situ* gamma spectrometer as a function of the photon energy for a homogeneous infinite plane surface contamination

D.2.1 Isotropic detector

The graphs in Figure D.2 indicate the fraction of the total number of photons detected that originate from within a certain radius from the detector. An isotropic detector is assumed where the ratio between crystal diameter and crystal height is about 1:1. The field-of-view of this *in situ* gamma spectrometer is characterized by the values at 90 % of gamma photons detected. The graphic shows that 90 % of the detected gamma photons at the energy of 60 keV come from an area with a radius of about 40 m, whereas the remaining 10 % come from a distance of more than 40 m, at the energy of 1 836 keV from more than about 60 m, respectively.

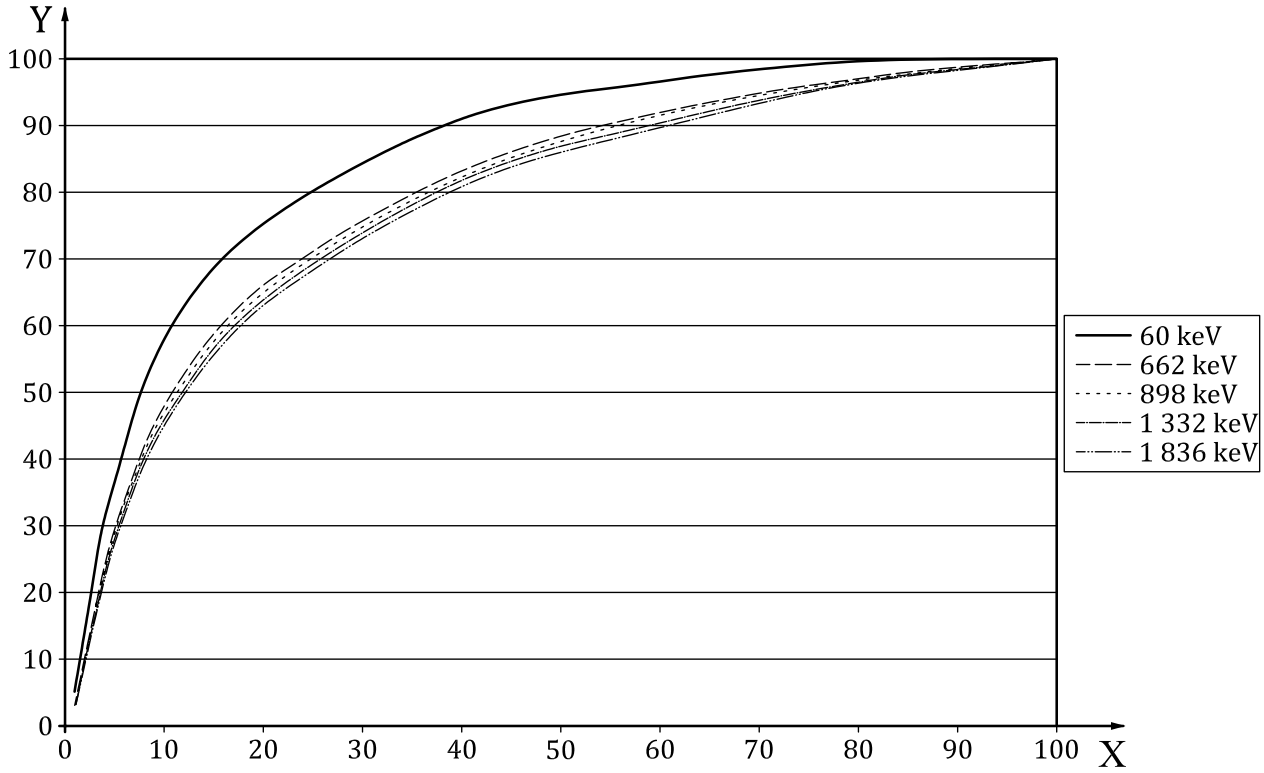

Key

X radius in m

Y percentage of gamma photons detected

Figure D.2 — Detector response as a function of the photon energy for a homogeneous infinite plane surface contamination in case of an isotropic detector

D.2.2 Non-isotropic detector

The following curves (see Figure D.3) indicate the percentage of gamma photons detected compared to the total number of gamma photons emitted from a surface contamination. In this case, a non-isotropic detector is assumed with a strong direction dependency where the ratio between crystal diameter and crystal height is about 2:1. The field-of-view of this *in situ* gamma spectrometer is characterized by the values at 90 % of gamma photons detected. In this case, the graphic shows that 90 % of the detected gamma photons at the energy of 60 keV come from an area with a radius of about 15 m, whereas the remaining 10 % come from a distance of more than 15 m, at 1 836 keV more than 55 m. This value of the distance at 1 836 keV is similar to that of an isotropic detector.

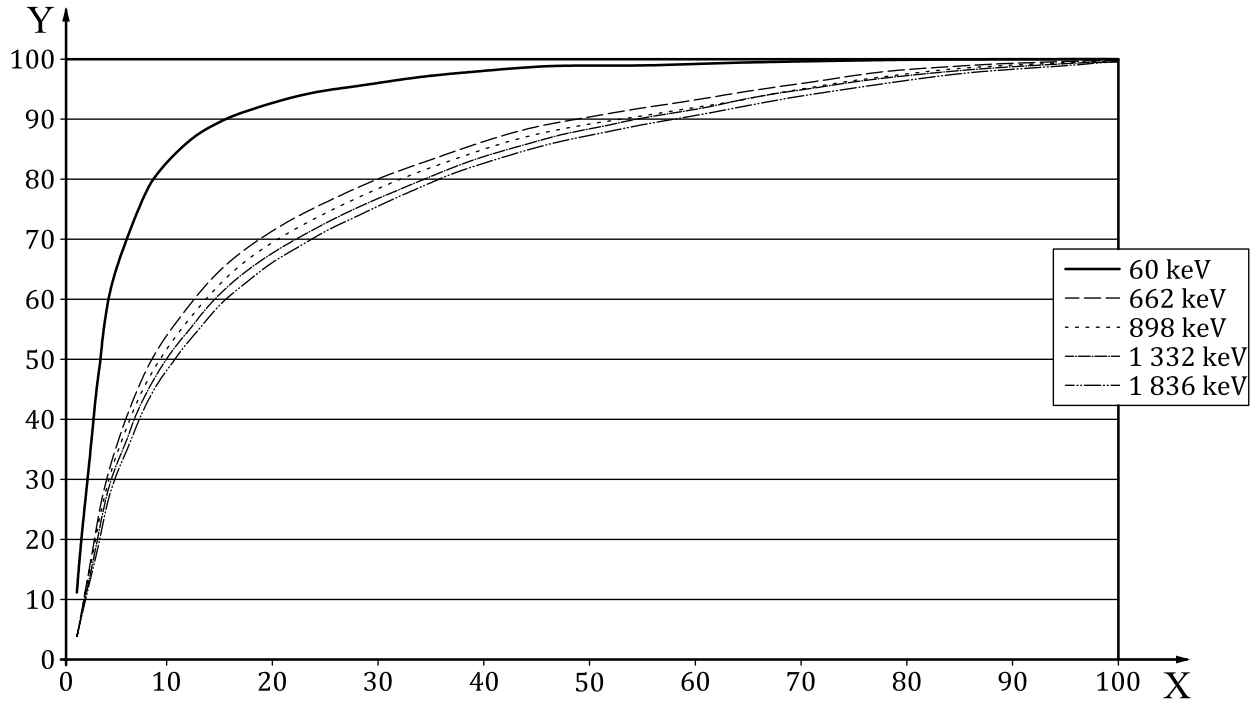

Key

X radius in m

Y percentage of gamma photons detected

Figure D.3 — Detector response as a function of the photon energy for a homogeneous infinite plane surface contamination in case of a non-isotropic detector

D.3 Field-of-view of an *in situ* gamma spectrometer with collimator as a function of the photon energy for different radionuclide distributions in soil

In Figure D.4, the field-of-view of an *in situ* gamma spectrometer is shown for different photon energies of the surface distribution of the radionuclides and use of a collimator. A lead collimator with 5 cm thickness, 10 cm diameter, and 90° conus is used. The figure shows the dependency of the normalized amount of unscattered photons from $\beta = 0$ constant specific activity and different sizes of the contaminated area. The aperture angle of the collimator is determined for the photon energy of 661,6 keV.

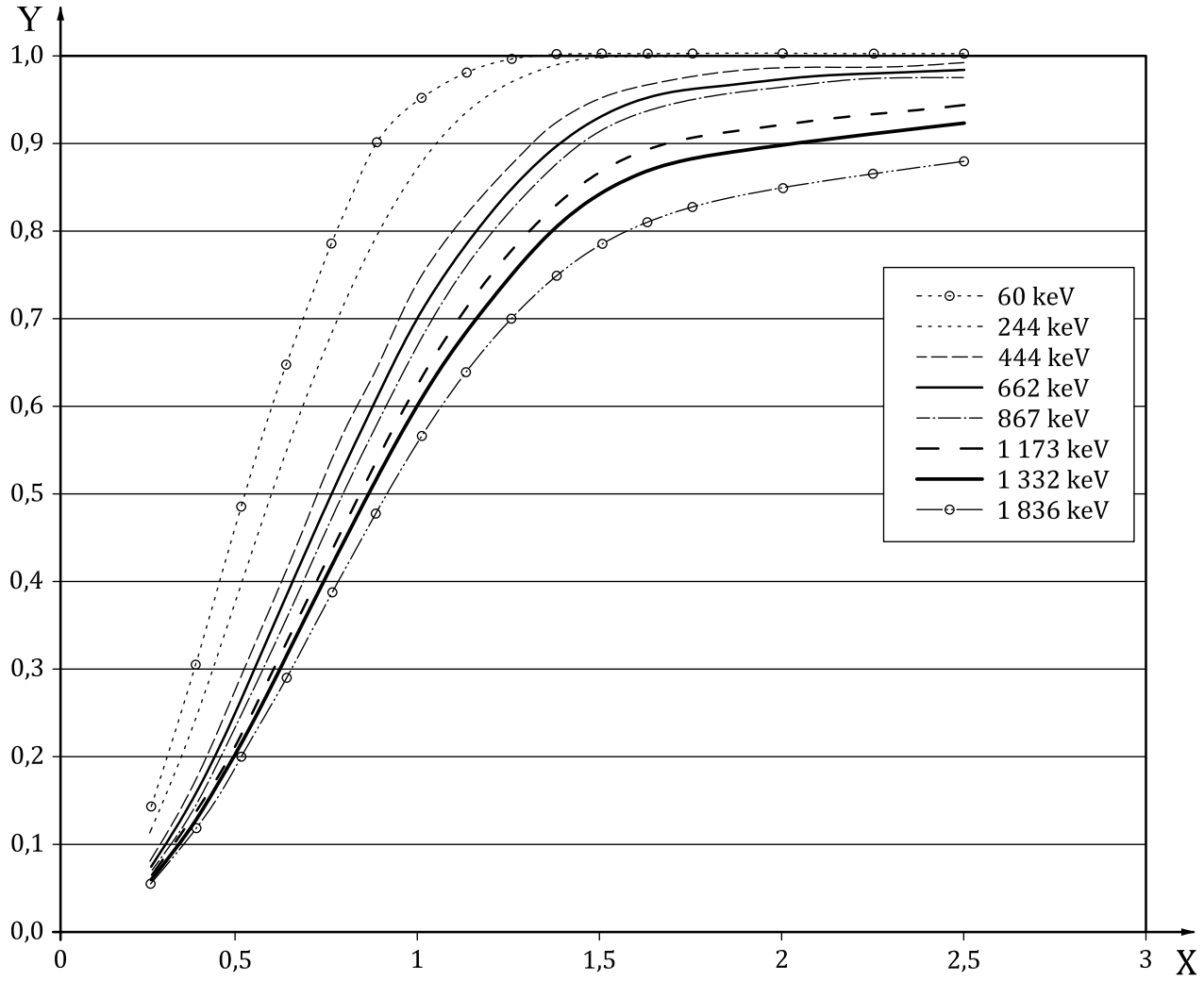

Key

X radius in m

Y percentage of gamma photons detected

Figure D.4 — Detector response as a function of the photon energy for a homogeneous finite plane surface contamination

Annex E
(informative)

Methods for calculating geometry factors and angular correction factors

NOTE See Reference [13].

The geometry function $G(E,V)$ for distribution V describes the ratio between the density of unscattered photon flux at the detector location and the intensity of the photon source per unit of surface area and/or mass under study. $G(E,V)$ is expressed as a function of the photon energy, the distribution of radionuclides in soil, and the height of the detector. The distribution of radionuclides in soil and/or on the ground surface is described by a mathematical model.

E.1 Geometry functions for distribution models with infinite plane surfaces

The following geometry functions are valid for distribution models with infinite plane surfaces.

Deposits on the ground surface:

$$G(E,V) = \frac{1}{2} \cdot \mathrm{E}_1 \left[\mu_{Air} \cdot d\right] \tag{E.1}$$

Exponential distribution in soil:

$$G(E,V) = \frac{1}{2}\left[\mathrm{E}_1(\mu_{Air} \cdot d) - \exp\left(\frac{1/\beta}{\mu_S/\rho_S} \cdot \mu_{Air} \cdot d\right) \cdot \mathrm{E}_1\left(\left(1 + \frac{1/\beta}{\mu_S/\rho_S}\right) \cdot \mu_{Air} \cdot d\right)\right] \tag{E.2}$$

Homogeneous distribution in soil:

$$G(E,V) = \frac{1}{2 \cdot \mu_S/\rho_S} \cdot \mathrm{E}_2 \left[\mu_{Air} \cdot d\right] \tag{E.3}$$

E.2 Geometry functions for distribution models with finite plane surfaces

The distribution models shown below consider circular distributions with radius R. The detector is placed in the centre of this measurement area (the symmetry axis of the crystal should be perpendicular to the measurement area). This gives the following geometry functions:

Deposits on the ground surface:

$$G(E,V)=\frac{1}{2}\left[\mathrm{E}_1(\mu_{Air}\cdot d)-\mathrm{E}_1(\mu_{Air}\cdot d/\cos\vartheta_{\lim})\right] \tag{E.4}$$

Exponential distribution in soil:

$$G(E,V)=\frac{1}{2}\left[\mathrm{E}_1(\mu_{Air}\cdot d)-\exp\left(\mu_{Air}\cdot d\cdot\frac{1/\beta}{\mu_S/\rho_S}\right)\cdot\mathrm{E}_1\left(\mu_{Air}\cdot d\cdot\left(\frac{1/\beta}{\mu_S/\rho_S}+1\right)\right)\right.$$
$$\left.-\mathrm{E}_1(\mu_{Air}\cdot d/\cos\vartheta_{\lim})+\exp\left(\mu_{Air}\cdot d\cdot\frac{1/\beta}{\mu_S/\rho_S}\right)\cdot\mathrm{E}_1\left(\mu_{Air}\cdot d\cdot\left(\frac{1/\beta}{\mu_S/\rho_S}+d/\cos\vartheta_{\lim}\right)\right)\right] \tag{E.5}$$

Homogeneous distribution in soil:

$$G(E,V)=\frac{1}{2\mu_S/\rho_S}\left[\mathrm{E}_2(\mu_{Air}\cdot d)-\mathrm{E}_2(\mu_{Air}\cdot d/\cos\vartheta_{\lim})\cdot\cos\vartheta_{\lim}\right] \tag{E.6}$$

Where

$$\vartheta_{\lim}=\arctan\left(\frac{\mathrm{R}}{d}\right) \tag{E.7}$$

E.3 Geometry function of different distributions of radionuclides in soil as function of the photon energy

Figure E.1 shows the geometry functions for deposits on the ground surface (β = 0 kg · m^{-2}) and for different exponential radionuclide distributions in soil as a function of photon energy. The detector height is 1 m above ground. In this case, the distribution model with infinite plane surface is used. The soil mass attenuation factors (composition of soil[8]) and air attenuation factors are given in Annex H.

Values for energies below 100 keV strongly depend on element composition of soil. In Annex H, an indication of this dependency is given.

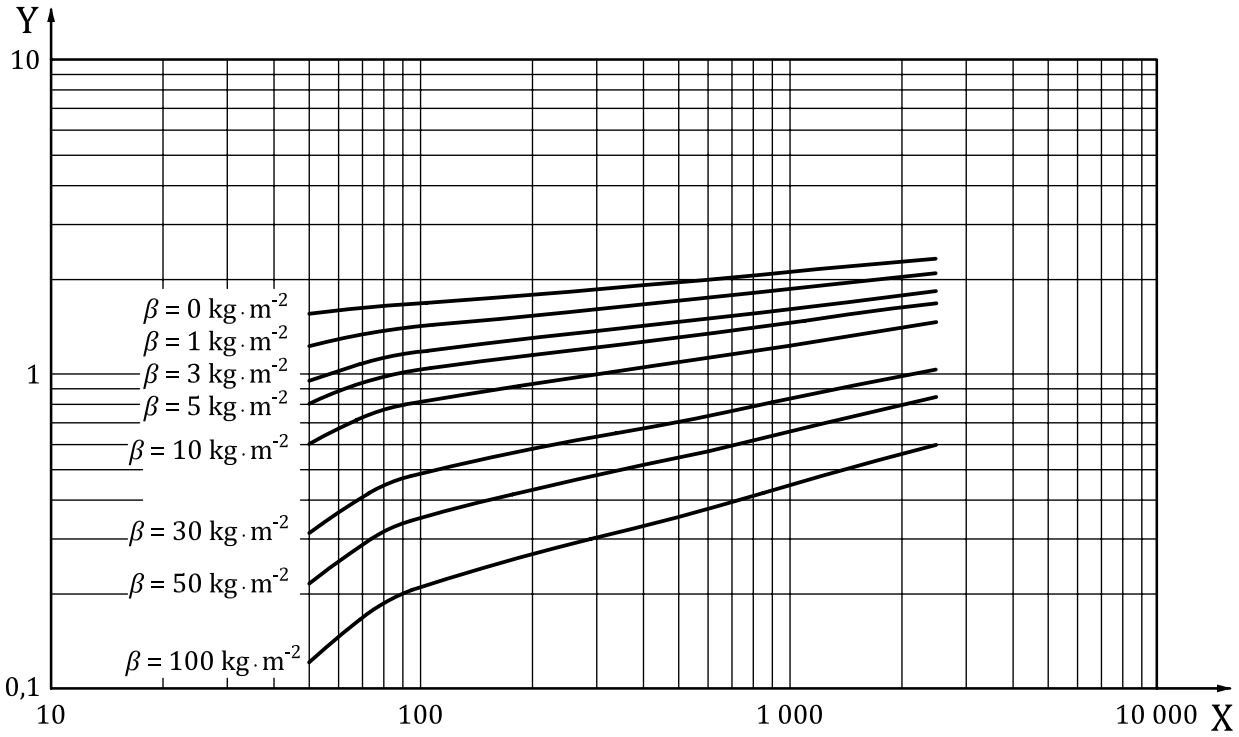

Key

X E in keV

Y $G(E, V)$

Figure E.1 — Geometry functions for deposits on the ground surface ($\beta = 0$ kg · m^{-2}) and for different exponential radionuclide distributions in soil as a function of photon energy (detector height at 1 m, relaxation mass per unit area, β, used as a parameter)

NOTE Due to deviations in the soil composition between these data and ICRU 53, there are remarkable differences (especially below 100 keV) in the order of 6 % at 60 keV for $\beta = 0$ kg·m^{-2}; see also Annex H.

E.4 Geometry function of homogeneous distribution of radionuclides in soil

Figure E.2 shows the geometry function for homogeneous distribution of radionuclides in soil as a function of photon energy. The detector height is 1 m. The distribution model assumes an infinite plane (ICRU 53 Chapter 3.1[7]). The mass attenuation factors for soil and for air are taken from Annex H.

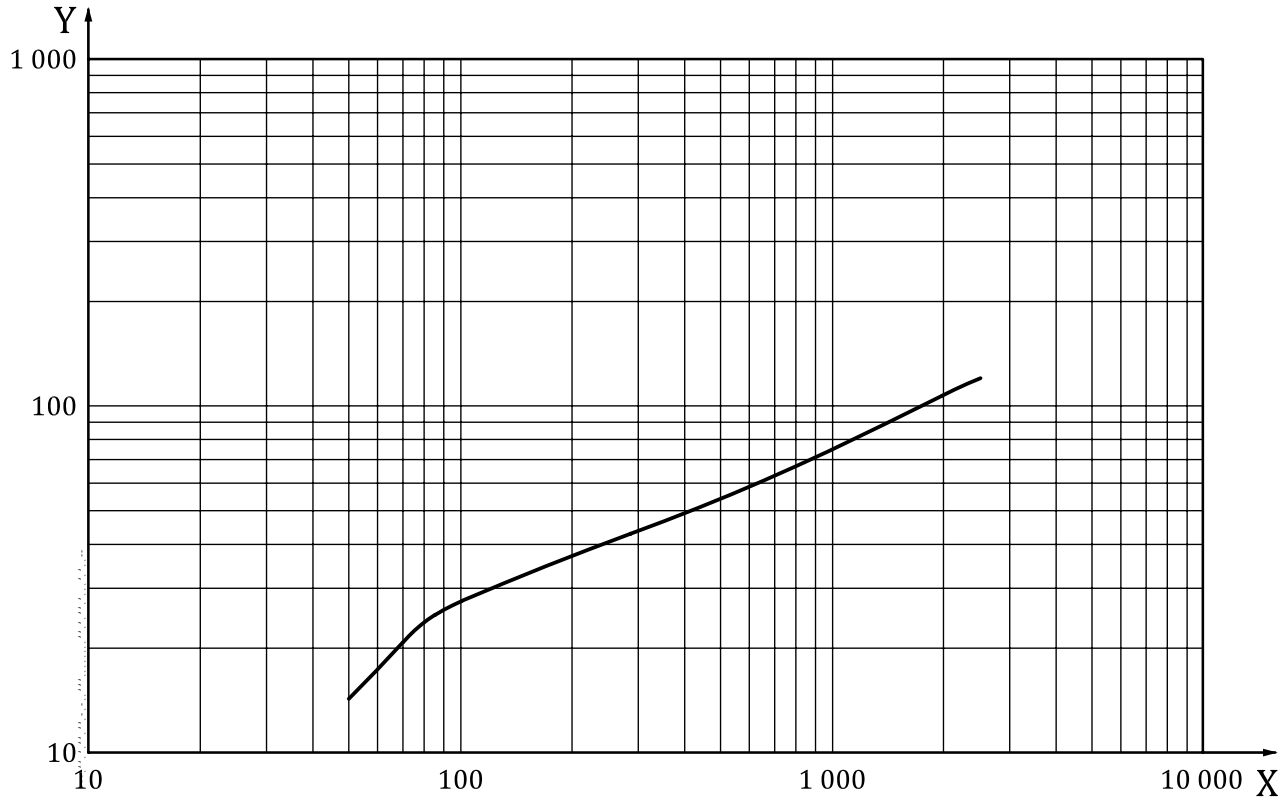

Key

X E in keV

Y $G(E, V)$ in kg · m^{-2}

Figure E.2 — Geometry function for homogeneous distribution of radionuclides in soil as a function of photon energy (detector height 1 m)

NOTE Due to deviations in the soil composition between these data and ICRU 53, there are remarkable differences (especially below 100 keV) in the order of 25 % at 60 keV for $\beta \rightarrow \infty$ kg·m^{-2}; see also Annex H.

E.5 Example for calculating the geometry factor for a measurement area with a finite plane surface

The following assumptions have been made for the calculations:

— measurement area 5 m × 5 m;

— detector placed in the centre of the measurement area, at a height of 1 m above the ground surface;

— deposit of ^{137}Cs (energy = 661,6 keV) at the ground surface (β = 0 kg·m^{-2});

— detector efficiency is not dependent on detector orientation.

For a distribution model with infinite plane, Formula (E.1) gives a geometry factor of 2. As the field-of-view of the *in situ* gamma spectrometer with radius R_S = 65 m is wider than the measurement area, the distribution model with infinite plane surfaces (see 6.2.2) shall not be used in this case.

If the geometry factor is calculated for the actual measurement geometry, i.e. a square measurement area with dimensions 5 m × 5 m (by a numerical method, for example), it yields a geometry factor of 0,53. If a distribution model with infinite plane surface is used, the activity calculated in relation to the measurement area would be underestimated by a factor of 4.

The geometry factor can be estimated for the current measurement geometry using Formula (E.4). The following value is obtained for a distribution model with radius *R*:

$$R = \sqrt{\frac{25m^2}{\pi}} = 2{,}8m \tag{E.8}$$

For a detector height of 1 m, the limit angle, $\vartheta_{\lim}$, is calculated as follows:

$$\vartheta_{\lim} = \arctan\left(\frac{R}{d}\right) = 70° \tag{E.9}$$

Formula (E.4) gives a geometry factor of 0,54. This value is close to the true geometry factor of the measurement area, which is 0,53.

For an *in situ* gamma spectrometer collimator, taking account of the specified conditions, the radius, R_S, of the field-of-view is approximately 1,6 m, which corresponds to a surface of approximately 8,1 m^2. Given that the field-of-view is narrower than the measurement area, the distribution model with infinite plane can be used as a basis for this calculation.

E.6 Calculation of flux density ratios for distribution models with infinite plane

The angular correction factor, *W*, has to be calculated, if there is a dependency of the detector efficiency from the polar angle, ϑ.

The calculation of the angular correction factor, *W*, contains the angular coefficient of the detector, k_m, and the flux density ratio, $\left(\frac{\Delta\Phi_m}{\Phi}\right)_{E,V}$. For distribution models with an infinite plane, the flux density ratios are given by the following formulae:

Deposits on the ground surface:

$$\left(\frac{\Delta\Phi_m}{\Phi}\right)_{E,V} = \frac{E_1(\mu_{Air} \cdot d/\cos\vartheta_{\text{int}}) - E_1(\mu_{Air} \cdot d/\cos\vartheta_{ext})}{E_1(\mu_{Air} \cdot d)} \tag{E.10}$$

Exponential distribution in soil:

$$\left(\frac{\Delta\Phi_m}{\Phi}\right)_{E,V} = \frac{\mathrm{E}_1(\mu_{Air} \cdot d/\cos\vartheta_{\text{int}}) - \exp\left(\mu_{Air} \cdot d \cdot \frac{1/\beta}{\mu_S/\rho_S}\right) \cdot \mathrm{E}_1\left(\mu_{Air} \cdot d \cdot \left(\frac{1/\beta}{\mu_S/\rho_S} + d/\cos\vartheta_{\text{int}}\right)\right)}{\mathrm{E}_1(\mu_{Air} \cdot d) - \exp\left(\mu_{Air} \cdot d \cdot \frac{1/\beta}{\mu_S/\rho_S}\right) \cdot \mathrm{E}_1\left(\mu_{Air} \cdot d \cdot \left(\frac{1/\beta}{\mu_S/\rho_S} + 1\right)\right)}$$

$$- \frac{\mathrm{E}_1(\mu_{Air} \cdot d/\cos\vartheta_{\text{ext}}) - \exp\left(\mu_{Air} \cdot d \cdot \frac{1/\beta}{\mu_S/\rho_S}\right) \cdot \mathrm{E}_1\left(\mu_{Air} \cdot d \cdot \left(\frac{1/\beta}{\mu_S/\rho_S} + d/\cos\vartheta_{\text{ext}}\right)\right)}{\mathrm{E}_1(\mu_{Air} \cdot d) - \exp\left(\mu_{Air} \cdot d \cdot \frac{1/\beta}{\mu_S/\rho_S}\right) \cdot \mathrm{E}_1\left(\mu_{Air} \cdot d \cdot \left(\frac{1/\beta}{\mu_S/\rho_S} + 1\right)\right)} \tag{E.11}$$

Uniform distribution in soil:

$$\left(\frac{\Delta\Phi_m}{\Phi}\right)_{E,V} = \frac{\mathrm{E}_2(\mu_{Air} \cdot d/\cos\vartheta_{\text{int}}) \cdot \cos\vartheta_{\text{int}} - \mathrm{E}_2(\mu_{Air} \cdot d/\cos\vartheta_{ext}) \cdot \cos\vartheta_{ext}}{\mathrm{E}_2(\mu_{Air} \cdot d)} \tag{E.12}$$

E.7 Calculation of flux density ratios for distribution models with a finite plane

The angular correction factor, W, has to be calculated, if there is a direction dependence of the detector efficiency from the polar angle, ϑ. The calculation of the angular correction factor, W, contains the angular coefficient of the detector, k_m, and the flux density ratio, $\left(\frac{\Delta\Phi_m}{\Phi}\right)_{E,V}$.

Circular distributions with radius R apply to all the model geometries given below. The detector is placed in the centre of this measurement area (the symmetry axis of the crystal should be perpendicular to the measurement area).

For distribution models with a finite plane, the flux density ratios are given by the following formulae:

Deposits on the ground surface:

$$\left(\frac{\Delta\Phi_m}{\Phi}\right)_{E,V} = \frac{E_1(\mu_{Air}\cdot d/\cos\vartheta_{int}) - E_1(\mu_{Air}\cdot d/\cos\vartheta_{ext})}{E_1(\mu_{Air}\cdot d) - E_1(\mu_{Air}\cdot d/\cos\vartheta_{lim})} \tag{E.13}$$

Exponential distribution in soil:

$$\left(\frac{\Delta\Phi_m}{\Phi}\right)_{E,V} = \frac{E_1(\mu_{Air}\cdot d/\cos\vartheta_{int}) - \exp\left(\mu_{Air}\cdot d\cdot\frac{1/\beta}{\mu_S/\rho_S}\right)\cdot E_1\left(\mu_{Air}\cdot d\cdot\left(\frac{1/\beta}{\mu_S/\rho_S}+1/\cos\vartheta_{int}\right)\right)}{E_1(\mu_{Air}\cdot d) - \exp\left(\mu_{Air}\cdot d\cdot\frac{1/\beta}{\mu_S/\rho_S}\right)\cdot E_1\left(\mu_{Air}\cdot d\cdot\left(\frac{1/\beta}{\mu_S/\rho_S}+1\right)\right) - E_1(\mu_{Air}\cdot d/\cos\vartheta_{lim}) + \exp\left(\mu_{Air}\cdot d\cdot\frac{1/\beta}{\mu_S/\rho_S}\right)\cdot E_1\left(\mu_{Air}\cdot d\left(\frac{1/\beta}{\mu_S/\rho_S}+1/\cos\vartheta_{lim}\right)\right)}$$
$$- \frac{E_1(\mu_{Air}\cdot d/\cos\vartheta_{ext}) - \exp\left(\mu_{Air}\cdot d\cdot\frac{1/\beta}{\mu_S/\rho_S}\right)\cdot E_1\left(\mu_{Air}\cdot d\left(\frac{1/\beta}{\mu_S/\rho_S}+1/\cos\vartheta_{ext}\right)\right)}{E_1(\mu_{Air}\cdot d) - \exp\left(\mu_{Air}\cdot d\cdot\frac{1/\beta}{\mu_S/\rho_S}\right)\cdot E_1\left(\mu_{Air}\cdot d\cdot\left(\frac{1/\beta}{\mu_S/\rho_S}+1\right)\right) - E_1(\mu_{Air}\cdot d/\cos\vartheta_{lim}) + \exp\left(\mu_{Air}\cdot d\cdot\frac{1/\beta}{\mu_S/\rho_S}\right)\cdot E_1\left(\mu_{Air}\cdot d\left(\frac{1/\beta}{\mu_S/\rho_S}+1/\cos\vartheta_{lim}\right)\right)} \tag{E.14}$$

Uniform distribution in soil:

$$\left(\frac{\Delta\Phi_m}{\Phi}\right)_{E,V} = \frac{E_2(\mu_{Air}\cdot d/\cos\vartheta_{int})\cdot\cos\vartheta_{int} - E_2(\mu_{Air}\cdot d/\cos\vartheta_{ext})\cdot\cos\vartheta_{ext}}{E_2(\mu_{Air}\cdot d) - E_2(\mu_{Air}\cdot d/\cos\vartheta_{lim})\cdot\cos\vartheta_{lim}} \tag{E.15}$$

Where

$$\vartheta_{lim} = \arctan\left(\frac{R}{d}\right) \tag{E.16}$$

and

$$\vartheta_{int} < \vartheta_{ext} \leq \vartheta_{lim} \tag{E.17}$$

E.8 Example of the calculation of the angular correction factor, *w*, for in situ gamma spectrometer without collimator

An exponential distribution of ^{137}Cs in soil (relaxation mass per unit area β = 10 kg · m^{-2}) is assumed. The angular correction factor, W, for the photon energy of ^{137}Cs at 661,6 keV is calculated according to Formula (6) using a summation algorithm.

The flux density ratios, $\left(\frac{\Delta\Phi_m}{\Phi}\right)_{E,V}$, as given in Table E.1 are calculated according to Formula (E.11) with the following parameters:

E = 661,6 keV, m = 9, β = 10 kg · m^{-2}, $R\rightarrow\infty$, d = 1 m

The mass attenuation coefficients of soil and air are taken from Annex H. The angular coefficients are determined by measurements according to 6.2.

Table E.1 — Example for the calculation of the angular correction factor, *W*, for an *in situ* gamma spectrometer without collimator

m	ϑ_{int} Degree	ϑ_{ext} Degree	$\left(\frac{\Delta\Phi_m}{\Phi}\right)_{E,V}$	k_m	$k_m \cdot \left(\frac{\Delta\Phi_m}{\Phi}\right)_{E,V}$	$\sum k_m \cdot \left(\frac{\Delta\Phi_m}{\Phi}\right)_{E,V}$
1	0	10	$6{,}14 \cdot 10^{-3}$	1	$6{,}14 \cdot 10^{-3}$	$6{,}14 \cdot 10^{-3}$
2	10	20	$1{,}87 \cdot 10^{-2}$	1,03	$1{,}93 \cdot 10^{-2}$	$2{,}54 \cdot 10^{-2}$
3	20	30	$3{,}24 \cdot 10^{-2}$	1,08	$3{,}50 \cdot 10^{-2}$	$6{,}04 \cdot 10^{-2}$
4	30	40	$4{,}83 \cdot 10^{-2}$	1,15	$5{,}55 \cdot 10^{-2}$	$1{,}16 \cdot 10^{-1}$
5	40	50	$6{,}85 \cdot 10^{-2}$	1,25	$8{,}56 \cdot 10^{-2}$	$2{,}02 \cdot 10^{-1}$
6	50	60	$9{,}46 \cdot 10^{-2}$	1,20	$1{,}14 \cdot 10^{-1}$	$3{,}16 \cdot 10^{-1}$
7	60	70	$1{,}36 \cdot 10^{-1}$	1,18	$1{,}60 \cdot 10^{-1}$	$4{,}76 \cdot 10^{-1}$
8	70	80	$2{,}14 \cdot 10^{-1}$	1,15	$2{,}46 \cdot 10^{-1}$	$7{,}22 \cdot 10^{-1}$
9	80	90	$3{,}81 \cdot 10^{-1}$	1,13	$4{,}31 \cdot 10^{-1}$	1,15

The angular correction factor, *W*, is 1,15.

E.9 Examples of the numerical calculation of the angular correction factor, W, for an in situ gamma spectrometer with collimator

An exponential distribution of ^{137}Cs in soil (relaxation mass per unit area β = 10 kg · m^{-2}) is assumed. The angular correction factor, *W*, for the photon energy of ^{137}Cs at 661,6 keV is calculated according to Formula (6) using a summation algorithm.

The flux density ratios, $\left(\frac{\Delta\Phi_m}{\Phi}\right)_{E,V}$, as given in Table E.2 are calculated according to Formula (E.14) with the following parameters:

E = 661,6 keV, m = 18, β = 10 kg · m^{-2}, $R \to \infty$, d = 1 m

The mass attenuation coefficients of soil and air are taken from Annex H. The angular coefficients are determined by measurements according to 6.2.

Table E.2 — Example for the calculation of the angular correction factor, *W*, for an *in situ* gamma spectrometer with collimator

m	ϑ_{int} Degree	ϑ_{ext} Degree	$\left(\frac{\Delta\Phi_m}{\Phi}\right)_{E,V}$	k_m	$k_m \cdot \left(\frac{\Delta\Phi_m}{\Phi}\right)_{E,V}$	$\sum k_m \cdot \left(\frac{\Delta\Phi_m}{\Phi}\right)_{E,V}$
1	0	5	$1{,}53 \cdot 10^{-3}$	1	$1{,}53 \cdot 10^{-3}$	$1{,}53 \cdot 10^{-3}$
2	5	10	$4{,}60 \cdot 10^{-3}$	1	$4{,}60 \cdot 10^{-3}$	$6{,}13 \cdot 10^{-3}$
3	10	15	$7{,}74 \cdot 10^{-3}$	1	$7{,}74 \cdot 10^{-3}$	$1{,}39 \cdot 10^{-2}$
4	15	20	$1{,}10 \cdot 10^{-2}$	1	$1{,}10 \cdot 10^{-2}$	$2{,}49 \cdot 10^{-2}$
5	20	25	$1{,}44 \cdot 10^{-2}$	0,99	$1{,}35 \cdot 10^{-2}$	$3{,}84 \cdot 10^{-2}$
6	25	30	$1{,}80 \cdot 10^{-2}$	0,97	$1{,}75 \cdot 10^{-2}$	$5{,}59 \cdot 10^{-2}$
7	30	35	$2{,}19 \cdot 10^{-2}$	0,90	$1{,}97 \cdot 10^{-2}$	$7{,}56 \cdot 10^{-2}$
8	35	40	$2{,}63 \cdot 10^{-2}$	0,81	$2{,}13 \cdot 10^{-2}$	$9{,}69 \cdot 10^{-2}$

Table E.2 *(continued)*

m	ϑ_{int} Degree	ϑ_{ext} Degree	$\left(\frac{\Delta\Phi_m}{\Phi}\right)_{E,V}$	k_m	$k_m \cdot \left(\frac{\Delta\Phi_m}{\Phi}\right)_{E,V}$	$\sum k_m \cdot \left(\frac{\Delta\Phi_m}{\Phi}\right)_{E,V}$
9	40	45	$3{,}11 \cdot 10^{-2}$	0,68	$2{,}11 \cdot 10^{-2}$	$1{,}18 \cdot 10^{-1}$
10	45	50	$3{,}67 \cdot 10^{-2}$	0,51	$1{,}87 \cdot 10^{-2}$	$1{,}34 \cdot 10^{-1}$
11	50	55	$4{,}33 \cdot 10^{-2}$	0,30	$1{,}30 \cdot 10^{-2}$	$1{,}50 \cdot 10^{-1}$
12	55	60	$5{,}13 \cdot 10^{-2}$	0,13	$6{,}67 \cdot 10^{-3}$	$1{,}56 \cdot 10^{-1}$
13	60	65	$6{,}13 \cdot 10^{-2}$	0,034	$2{,}08 \cdot 10^{-3}$	$1{,}58 \cdot 10^{-1}$
14	65	70	$7{,}46 \cdot 10^{-2}$	0,009	$6{,}71 \cdot 10^{-4}$	$1{,}59 \cdot 10^{-1}$
15	70	75	$9{,}31 \cdot 10^{-2}$	0,008	$7{,}45 \cdot 10^{-4}$	$1{,}60 \cdot 10^{-1}$
16	75	80	$1{,}21 \cdot 10^{-1}$	0,009	$1{,}09 \cdot 10^{-3}$	$1{,}61 \cdot 10^{-1}$
17	80	85	$1{,}69 \cdot 10^{-1}$	0,01	$1{,}69 \cdot 10^{-3}$	$1{,}63 \cdot 10^{-1}$
18	85	90	$2{,}12 \cdot 10^{-4}$	0,01	$2{,}12 \cdot 10^{-3}$	$1{,}65 \cdot 10^{-1}$

The angular correction factor, W, is 0,165.

Annex F
(informative)

Example for calculation of the characteristic limits as well as the best estimate of the measurand and its standard uncertainty

F.1 Introduction

A p-type high-performance detector with a relative efficiency of 39 % and a relation of crystal diameter to crystal length of 1,034 (according detector specification) is located on a tripod at 1 m above ground. The area under survey is approximately plane and the extension is so large that an infinite plane surface is assumed for the distribution model. The growth is short; the area has only a few trees. The calculation model (Annex E) can be used.

In the following, the activity for ^{137}Cs is calculated in units of surface contamination. In a next step, the amount of radionuclide specific dose rate is calculated.

According to Formulae (4) and (8) in 6.2 and 8.1, the specific activity results in:

$$a = \frac{\left(n_g - n_b\right)/t}{p \cdot \eta_0 \cdot G \cdot W \cdot f_d} = w/t \cdot n_n \tag{F.1}$$

There are only two quantities associated with an uncertainty: the net count rate, n_n, of the peak and the calibration factor, w. It is assumed that the net counts of the peak and its uncertainty at the energy E is determined. Furthermore, one abandons a decay correction and the transition probability is not considered by the propagation of uncertainty. The related uncertainty results in [according to Formula (11) in 8.2.2]:

$$u(a) = \sqrt{w^2/t^2 \cdot u^2(n_n) + a^2 \cdot u_{rel}^2(w)} \tag{F.2}$$

NOTE Formulae (12) and (14) (8.2.3) illustrate that the uncertainty of the net count rate determines the decision threshold directly and the detection limit indirectly, while the uncertainty of the calibration factor affects exclusively the detection limit.

F.2 Determination of peak areas n_n, n_b and $u(n_n)$, $u(n_b)$

After = 3 000 seconds, the peak area result in $n_n \pm u\left(n_n\right)$ = 730 ± 32 counts for the energy line at 661,6 keV.

Concerning the calculation of the decision threshold and the detection limit, the term $n_b + u^2\left(n_b\right) = 2\, n_b$ is determined as 678.

F.3 Determination of w and $u(w)$

The values in this example are for the decay correction f_d = 1 and p = 0,85, as well as $u\left(f_d\right) = u\left(p\right) = 0$.

In case of the combined calibration procedure, the three factors η_0, G, and W, including the single standard uncertainty, have to be determined and reported.

Detector efficiency for this detector amounts to η_0 = (8,126±0,630) 10^{-4} m^2.

In general, the angular correction factor, W, is hard to determine. Because of the nearly angular independence of the detector for the important energies, the factor results in W = 0,982 ± 0,024 independent of the distribution model.

The geometry factor can be calculated according to Annex E or taken from literature. The geometry factor can be determined accurately within a few percent using appropriate programs, assuming the distribution model reflects the reality exactly. Because this is not the case in practice, the uncertainty of the geometry factor — especially for measurements in the field — includes the major systematic error.

Hereafter, it is assumed that the activity decreases with the depth like an exponential function. Additionally, one assumes that the parameter β with a lower limit of 5 g cm^{-2} (50 kg·m^{-2}) and an upper limit of 20 g·cm^{-2} (200 kg·m^{-2}) can be completely described.

The value for the geometry factor is taken from[7] and amounts to 0,530 for β = 5 g cm^{-2} (50 kg·m^{-2}) or 0,210 for β = 20 g·cm^{-2} (200 kg·m^{-2}).

If for the geometry factor — in contrast with the other quantities — a square wave distribution between the above mentioned values is taken as a basis, the corresponding standard uncertainty is calculated according to GUM as $u(G) = \Delta G / \sqrt{12}$.

For G defined as centre of the range follows: G = 0,370 ± 0,093.

NOTE According to Table A.1 in Reference [7], the geometry factor covers the photon emission probability already.

According to Formula (8) (see 8.1), the calibration factor arises as a result: w = (0,336 ± 0,089) 10^4 m^{-2}. The relative uncertainty $u_{rel}(w)$ ~26,5 % is determined completely from the relative uncertainty $u_{rel}(G)$ ~25,1 %.

F.4 Calculation of the decision threshold and detection limit

Given is a ^{137}Cs contamination of soil with an exponential distribution (β = 10 kg · m^{-2}). For an *in situ* gamma spectrometer with a detector of 39 % efficiency, the decision threshold and detection limit should be determined as activity per unit of surface area; a decay correction is not implemented.

For the calculation, the following parameters are used.

Background counts in the area of the peak at 661,6 keV:	$2n_b$ = 678; $n_b + u^2(n_b) = 2n_b$
Peak area:	$n_n \pm u(n_n)$ = 730 ± 32
Measuring time:	t = 3 000 s
Variable w (summation of all quantities):	w = (0,336 ± 0,089) 10^4 m^{-2}
Decay correction factor:	f_d = 1
Photon emission probability for the 661,6 keV line:	p = 0,851
Detector efficiency:	η_0 = (8,126 ± 0,630) 10^{-4} m^2
Relaxation mass per unit area:	50 < β < 200 kg · m^{-2}
Detector height:	d = 1,0 m
Quantiles of the standardized normal distribution:	$k_{1-\alpha} = k_{1-\beta} = k$ = 1,645
Geometry factor:	G = 0,370 ± 0,093
Angle correction factor W:	W = 0,982±0,024

Relative uncertainty of w: $u_{rel}(w) \sim 0{,}265$

Relative uncertainty of G: $u_{rel}(G) \sim 0{,}251$

The decision threshold, a^*, for the activity per unit of surface area is calculated according to Formula (12) (8.2)

$$a^* = k\sqrt{w^2 \cdot t^{-2} \cdot \left[n_b + u^2(n_b)\right]} = 1{,}645\sqrt{(0{,}336 \cdot 10^4)^2 \cdot 3000^{-2} \cdot 678} = 48\ Bq \cdot m^{-2}$$

The detection limit, $a^{\#}$, for the activity per unit of surface area is calculated according to Formula (13) and is equal to 122 Bq/m^2.

F.5 Calculation of the primary measurement result and its standard uncertainty

$$a = \frac{w}{t} \cdot n_n = (0{,}336 \cdot 10^4 \cdot 730)/3000 = 818\ Bq \cdot m^{-2}$$

$$u(a) = \sqrt{\frac{w^2}{t^2} \cdot (u^2(n_n) + a^2 \cdot u_{rel}^2(w))}$$

$$= \sqrt{\left(0{,}336 \cdot 10^4\right)^2 \cdot (3\,000)^{-2} \cdot (32)^2 + (818)^2 \cdot (0{,}265)^2} = \sqrt{(1\,283{,}2 + 46\,989{,}2)} = 220\ Bq \cdot m^{-2}$$

With $a/u(a)$ approximately 3,72, the approximation $\hat{a} = a$ and $u(\hat{a}) = u(a)$ is applied. The primary measuring result is interpreted as best estimate.

NOTE In the case at issue ω = 1 − 1,004·10^{-4}. The value for ω is calculated by EXCEL® with the function STANDNORMVALUE(x) where x = $a/u(a)$.

The upper limit of the confidence interval is calculated according to 8.2.4:

$a^{\triangleright} \sim 1\,180$ Bq·m^{-2}

Summary of results

Decision threshold: $a^* = 48$ Bq · m^{-2}

Detection limit: $a^{\#} = 122$ Bq · m^{-2}

Activity per unit of surface area: $a = (818 \pm 220)$ Bq · m^{-2}

F.6 Calculation of the radionuclide specific ambient dose equivalent rate

The statement of the primary measuring results as dose rate modifies the calibration factor, w, and its standard uncertainty, $u(w)$. In calculating the ambient dose equivalent rate, $\dot{H}^*(10)$, correction factors $f_{\dot{H}^*(10)}$ from[9,10] are used. The reciprocal value of the respective factors amount to 1,5 · 10^{-3} nSv · h^{-1} Bq^{-1} · m^2 for β = 50 g · cm^{-2} or 0,723 · 10^{-3} nSv · h^{-1} Bq^{-1} · m^2 for β = 200 kg·m^{-2} for both distribution models.

To calculate w_h and $u(w_h)$, the product $G \cdot f_{\dot{H}^*(10)}$ is generated according to Formula (20), using 0,353 · 10^3 Bq · m^{-2} · nSv^{-1} · h for β = 50 kg · m^{-2} or 0,290 · 10^3 Bq · m^{-2} · nSv^{-1} · h for β = 200 kg · m^{-2}. Analogous to the procedure above, the product results in $G \cdot f_{\dot{H}^*(10)} = (322{,}0 \pm 18) \cdot 10^3$ Bq · m^{-2} · nSv^{-1} · h.

The relative uncertainty is ~5,7 % and thus, within the range of other quantities or of the models itself. Hence, it amounts to w_h = (3,75±0,37) 10^{-3} nSv · h^{-1}. The relative uncertainty amounts to $u_{rel}(w_h)$ ~9,8 %.

NOTE 1 During the determination of the radionuclide specific dose rate, $u(G)$ and $u(f_D)$ are partly compensated for while considering different distribution models, if the built up-factor remains more or less constant.

Under this assumption, the decision threshold results in 54 · 10^{-3} nSv · h^{-1}, and the detection limit in 111 10^{-3} nSv · h^{-1}.

The primary measurement of the result and its uncertainty amounts to (913 ± 98) · 10^{-3} nSv · h^{-1}.

NOTE 2 Because of the small value of $u_{rel}(w_h)$, the relation between the decision threshold and the detection limit approximates the theoretical minimum of 2.

Summary of results

Relaxation mass per unit area:	$50 < \beta < 200$ kg · m^{-2}
Correction factor (activity to ambient dose rate):	$f_{\dot{H}^*(10)}$ = 1,5 10^{-3} nSv · h^{-1} Bq^{-1} · m^2 (for β = 50 kg · m^{-2})
	$f_{\dot{H}^*(10)}$ = 0,723 10^{-3} nSv · h^{-1} Bq^{-1} · m^2 (for β = 200 kg·m^{-2})
Calibration factor, w_h (ambient dose equivalent rate):	w_h = (3,75±0,37) · 10^{-3} nSv · h^{-1}
Decision threshold:	$\dot{H}^*(10)^*$ = 54 · 10^{-3} nSv · h^{-1}
Detection limit:	$\dot{H}^*(10)^\#$ = 11 · 10^{-3} nSv · h^{-1}
Ambient dose rate:	$\dot{H}^*(10)$ = (913 ± 98) · 10^{-3} nSv · h^{-1}

Annex G
(informative)

Conversion factors for surface or mass activity to air kerma rate and ambient dose equivalent rate for different radionuclide distribution in soil

Example is showing the calculation of dose rate using the measured activities of individual radionuclides.

G.1 Factor f_D to calculate the air kerma rate for natural radionuclides in case of uniform distribution in soil

Table G.1 contains the factors to convert the activity as unit of mass to air kerma rate at 1 m above ground for natural radionuclides in case of uniform distribution.

Table G.1 — Conversion factors for activity per unit of mass in terms of air kerma rate at 1 m above ground for natural radionuclides [case of uniform distribution] ($\beta \rightarrow \infty$ kg·m^{-2})[[7]]

Radionuclide	Factor f_D nGy · kg · h^{-1} · Bq^{-1}
Uranium / Radium series	
^{238}U	$4{,}33 \cdot 10^{-5}$
^{234}U	$5{,}14 \cdot 10^{-5}$
^{234}Th	$9{,}47 \cdot 10^{-4}$
^{234m}Pa	$3{,}00 \cdot 10^{-3}$
^{234}Pa	$4{,}49 \cdot 10^{-4}$
^{230}Th	$6{,}90 \cdot 10^{-5}$
^{226}Ra	$1{,}25 \cdot 10^{-3}$
^{222}Rn	$8{,}78 \cdot 10^{-5}$
^{214}Pb	$5{,}46 \cdot 10^{-2}$
^{214}Bi	$4{,}01 \cdot 10^{-1}$
^{210}Tl	$1{,}15 \cdot 10^{-4}$
^{210}Pb	$2{,}07 \cdot 10^{-4}$
Uranium series, total	$4{,}62 \cdot 10^{-1}$
Thorium series	
^{232}Th	$4{,}78 \cdot 10^{-5}$
^{228}Ra	$5{,}45 \cdot 10^{-5}$
^{228}Ac	$2{,}21 \cdot 10^{-1}$
^{228}Th	$3{,}44 \cdot 10^{-4}$
^{224}Ra	$2{,}14 \cdot 10^{-3}$
^{220}Rn	$1{,}73 \cdot 10^{-4}$
^{212}Pb	$2{,}77 \cdot 10^{-2}$
^{212}Bi	$2{,}72 \cdot 10^{-2}$

Table G.1 *(continued)*

Radionuclide	Factor f_D nGy · kg · h^{-1} · Bq^{-1}
^{208}Tl	$3{,}26 \cdot 10^{-1}$
Thorium series, total	$6{,}04 \cdot 10^{-1}$
^{40}K	$4{,}17 \cdot 10^{-2}$

G.2 Factor f_D to convert activity to air kerma rate for some relevant radionuclides at different relaxation masses per unit area, β.

Table G.2 contains the factors to convert the activity as unit of mass to air kerma rate at 1 m above ground for some relevant radionuclides at different relaxation masses per unit area, β.

Table G.2 — Factors to convert the activity of unit of mass to air kerma rate at 1 m above ground in case of different relaxation masses per unit area, β, from[[7]]

Radio-nuclide	Factor f_D in nGy · m^2 · h^{-1} · Bq^{-1} by relaxation mass per unit area, β, in kg · m^{-2}							
	0	1	3	5	10	20	50	100
^{7}Be	$2{,}26 \cdot 10^{-4}$	$2{,}04 \cdot 10^{-4}$	$1{,}81 \cdot 10^{-4}$	$1{,}67 \cdot 10^{-4}$	$1{,}46 \cdot 10^{-4}$	$1{,}22 \cdot 10^{-4}$	$8{,}77 \cdot 10^{-5}$	$6{,}28 \cdot 10^{-5}$
^{51}Cr	$2{,}18 \cdot 10^{-4}$	$1{,}47 \cdot 10^{-4}$	$1{,}20 \cdot 10^{-4}$	$1{,}09 \cdot 10^{-4}$	$9{,}39 \cdot 10^{-5}$	$7{,}77 \cdot 10^{-5}$	$5{,}55 \cdot 10^{-5}$	$3{,}95 \cdot 10^{-3}$
^{54}Mn	$3{,}71 \cdot 10^{-3}$	$3{,}30 \cdot 10^{-3}$	$2{,}92 \cdot 10^{-3}$	$2{,}69 \cdot 10^{-3}$	$2{,}35 \cdot 10^{-3}$	$1{,}97 \cdot 10^{-3}$	$1{,}43 \cdot 10^{-3}$	$1{,}04 \cdot 10^{-3}$
^{59}Fe	$4{,}87 \cdot 10^{-3}$	$4{,}42 \cdot 10^{-3}$	$3{,}93 \cdot 10^{-3}$	$3{,}64 \cdot 10^{-3}$	$3{,}18 \cdot 10^{-3}$	$2{,}67 \cdot 10^{-3}$	$1{,}96 \cdot 10^{-3}$	$1{,}43 \cdot 10^{-3}$
^{57}Co	$8{,}09 \cdot 10^{-4}$	$5{,}51 \cdot 10^{-4}$	$4{,}35 \cdot 10^{-4}$	$3{,}88 \cdot 10^{-4}$	$3{,}28 \cdot 10^{-4}$	$2{,}65 \cdot 10^{-4}$	$1{,}80 \cdot 10^{-4}$	$1{,}22 \cdot 10^{-4}$
^{58}Co	$4{,}38 \cdot 10^{-3}$	$3{,}89 \cdot 10^{-3}$	$3{,}44 \cdot 10^{-3}$	$3{,}17 \cdot 10^{-3}$	$2{,}77 \cdot 10^{-3}$	$2{,}32 \cdot 10^{-3}$	$1{,}69 \cdot 10^{-3}$	$1{,}22 \cdot 10^{-3}$
^{60}Co	$1{,}02 \cdot 10^{-2}$	$9{,}20 \cdot 10^{-3}$	$8{,}18 \cdot 10^{-3}$	$7{,}59 \cdot 10^{-3}$	$6{,}64 \cdot 10^{-3}$	$5{,}58 \cdot 10^{-3}$	$4{,}10 \cdot 10^{-3}$	$3{,}00 \cdot 10^{-3}$
^{65}Zn	$2{,}62 \cdot 10^{-3}$	$2{,}26 \cdot 10^{-3}$	$1{,}97 \cdot 10^{-3}$	$1{,}82 \cdot 10^{-3}$	$1{,}58 \cdot 10^{-3}$	$1{,}33 \cdot 10^{-3}$	$9{,}70 \cdot 10^{-4}$	$7{,}07 \cdot 10^{-4}$
^{91}Y	$1{,}48 \cdot 10^{-5}$	$1{,}34 \cdot 10^{-5}$	$1{,}19 \cdot 10^{-5}$	$1{,}10 \cdot 10^{-5}$	$9{,}64 \cdot 10^{-6}$	$8{,}10 \cdot 10^{-6}$	$5{,}94 \cdot 10^{-6}$	$4{,}35 \cdot 10^{-6}$
^{95}Zr	$3{,}23 \cdot 10^{-3}$	$2{,}93 \cdot 10^{-3}$	$2{,}60 \cdot 10^{-3}$	$2{,}40 \cdot 10^{-3}$	$2{,}10 \cdot 10^{-3}$	$1{,}76 \cdot 10^{-3}$	$1{,}28 \cdot 10^{-3}$	$9{,}25 \cdot 10^{-4}$
^{97}Zr	$8{,}21 \cdot 10^{-4}$	$7{,}39 \cdot 10^{-4}$	$6{,}55 \cdot 10^{-4}$	$6{,}06 \cdot 10^{-4}$	$5{,}92 \cdot 10^{-4}$	$4{,}43 \cdot 10^{-4}$	$3{,}23 \cdot 10^{-4}$	$2{,}35 \cdot 10^{-4}$
^{95}Nb	$3{,}35 \cdot 10^{-3}$	$3{,}03 \cdot 10^{-3}$	$2{,}69 \cdot 10^{-3}$	$2{,}49 \cdot 10^{-3}$	$2{,}17 \cdot 10^{-3}$	$1{,}82 \cdot 10^{-3}$	$1{,}32 \cdot 10^{-3}$	$9{,}59 \cdot 10^{-4}$
^{97}Nb	$2{,}97 \cdot 10^{-3}$	$2{,}68 \cdot 10^{-3}$	$2{,}39 \cdot 10^{-3}$	$2{,}21 \cdot 10^{-3}$	$1{,}92 \cdot 10^{-3}$	$1{,}61 \cdot 10^{-3}$	$1{,}17 \cdot 10^{-3}$	$8{,}44 \cdot 10^{-4}$
^{99}Mo	$6{,}54 \cdot 10^{-4}$	$5{,}29 \cdot 10^{-4}$	$5{,}26 \cdot 10^{-4}$	$4{,}85 \cdot 10^{-4}$	$4{,}23 \cdot 10^{-4}$	$3{,}54 \cdot 10^{-4}$	$2{,}56 \cdot 10^{-4}$	$1{,}84 \cdot 10^{-4}$
^{99m}Tc	$5{,}66 \cdot 10^{-4}$	$4{,}93 \cdot 10^{-4}$	$4{,}30 \cdot 10^{-4}$	$3{,}93 \cdot 10^{-4}$	$3{,}40 \cdot 10^{-4}$	$2{,}79 \cdot 10^{-4}$	$1{,}93 \cdot 10^{-4}$	$1{,}32 \cdot 10^{-4}$
^{103}Ru	$2{,}21 \cdot 10^{-3}$	$2{,}00 \cdot 10^{-3}$	$1{,}77 \cdot 10^{-3}$	$1{,}64 \cdot 10^{-3}$	$1{,}43 \cdot 10^{-3}$	$1{,}19 \cdot 10^{-3}$	$8{,}59 \cdot 10^{-4}$	$6{,}16 \cdot 10^{-4}$
^{105}Ru	$3{,}35 \cdot 10^{-3}$	$3{,}00 \cdot 10^{-3}$	$2{,}65 \cdot 10^{-3}$	$2{,}45 \cdot 10^{-3}$	$2{,}13 \cdot 10^{-3}$	$1{,}78 \cdot 10^{-3}$	$1{,}29 \cdot 10^{-3}$	$9{,}28 \cdot 10^{-4}$
^{103m}Rh	$4{,}43 \cdot 10^{-4}$	$2{,}35 \cdot 10^{-4}$	$1{,}27 \cdot 10^{-4}$	$8{,}82 \cdot 10^{-5}$	$5{,}05 \cdot 10^{-5}$	$2{,}75 \cdot 10^{-5}$	$1{,}16 \cdot 10^{-5}$	$5{,}93 \cdot 10^{-6}$
^{105}Rh	$3{,}53 \cdot 10^{-4}$	$3{,}19 \cdot 10^{-4}$	$2{,}83 \cdot 10^{-4}$	$2{,}62 \cdot 10^{-4}$	$2{,}28 \cdot 10^{-4}$	$1{,}90 \cdot 10^{-4}$	$1{,}36 \cdot 10^{-4}$	$9{,}71 \cdot 10^{-5}$
^{106}Rh	$9{,}30 \cdot 10^{-4}$	$8{,}40 \cdot 10^{-4}$	$7{,}46 \cdot 10^{-4}$	$6{,}90 \cdot 10^{-4}$	$6{,}02 \cdot 10^{-4}$	$5{,}03 \cdot 10^{-4}$	$2{,}65 \cdot 10^{-4}$	$2{,}63 \cdot 10^{-4}$
^{110m}Ag	$1{,}18 \cdot 10^{-2}$	$1{,}06 \cdot 10^{-2}$	$9{,}46 \cdot 10^{-3}$	$8{,}76 \cdot 10^{-3}$	$7{,}64 \cdot 10^{-3}$	$6{,}41 \cdot 10^{-3}$	$4{,}68 \cdot 10^{-3}$	$3{,}40 \cdot 10^{-3}$
^{124}Sb	$7{,}58 \cdot 10^{-3}$	$6{,}86 \cdot 10^{-3}$	$6{,}12 \cdot 10^{-3}$	$5{,}67 \cdot 10^{-3}$	$4{,}95 \cdot 10^{-3}$	$4{,}16 \cdot 10^{-3}$	$3{,}05 \cdot 10^{-3}$	$2{,}23 \cdot 10^{-3}$
^{125}Sb	$2{,}15 \cdot 10^{-3}$	$1{,}87 \cdot 10^{-3}$	$1{,}62 \cdot 10^{-3}$	$1{,}48 \cdot 10^{-3}$	$1{,}27 \cdot 10^{-3}$	$1{,}05 \cdot 10^{-3}$	$7{,}52 \cdot 10^{-4}$	$5{,}37 \cdot 10^{-4}$
^{127}Sb	$2{,}97 \cdot 10^{-3}$	$2{,}68 \cdot 10^{-3}$	$2{,}38 \cdot 10^{-3}$	$2{,}20 \cdot 10^{-3}$	$1{,}92 \cdot 10^{-3}$	$1{,}60 \cdot 10^{-3}$	$1{,}16 \cdot 10^{-3}$	$8{,}35 \cdot 10^{-4}$
^{129}Sb	$6{,}14 \cdot 10^{-3}$	$5{,}56 \cdot 10^{-3}$	$4{,}94 \cdot 10^{-3}$	$4{,}58 \cdot 10^{-3}$	$4{,}00 \cdot 10^{-3}$	$3{,}35 \cdot 10^{-3}$	$2{,}45 \cdot 10^{-3}$	$1{,}78 \cdot 10^{-3}$

Table G.2 *(continued)*

Radio-nuclide	Factor f_D in nGy · m^2 · h^{-1} · Bq^{-1} by relaxation mass per unit area, β, in kg · m^{-2}							
	0	1	3	5	10	20	50	100
^{130}Sb	$1{,}41 \cdot 10^{-2}$	$1{,}27 \cdot 10^{-2}$	$1{,}13 \cdot 10^{-2}$	$1{,}04 \cdot 10^{-2}$	$9{,}12 \cdot 10^{-3}$	$7{,}64 \cdot 10^{-3}$	$5{,}56 \cdot 10^{-3}$	$4{,}02 \cdot 10^{-3}$
^{127}Te	$2{,}26 \cdot 10^{-5}$	$2{,}03 \cdot 10^{-5}$	$1{,}79 \cdot 10^{-5}$	$1{,}65 \cdot 10^{-5}$	$1{,}44 \cdot 10^{-5}$	$1{,}20 \cdot 10^{-5}$	$8{,}58 \cdot 10^{-6}$	$6{,}12 \cdot 10^{-6}$
^{127m}Te	$2{,}09 \cdot 10^{-4}$	$1{,}25 \cdot 10^{-4}$	$7{,}80 \cdot 10^{-5}$	$5{,}91 \cdot 10^{-5}$	$3{,}78 \cdot 10^{-5}$	$2{,}25 \cdot 10^{-5}$	$1{,}03 \cdot 10^{-5}$	$5{,}48 \cdot 10^{-6}$
^{129}Te	$3{,}45 \cdot 10^{-4}$	$2{,}77 \cdot 10^{-4}$	$2{,}30 \cdot 10^{-4}$	$2{,}07 \cdot 10^{-4}$	$1{,}75 \cdot 10^{-4}$	$1{,}42 \cdot 10^{-4}$	$1{,}00 \cdot 10^{-4}$	$7{,}12 \cdot 10^{-5}$
^{129m}Te	$3{,}71 \cdot 10^{-4}$	$2{,}63 \cdot 10^{-4}$	$1{,}95 \cdot 10^{-4}$	$1{,}65 \cdot 10^{-4}$	$1{,}28 \cdot 10^{-4}$	$9{,}62 \cdot 10^{-5}$	$6{,}29 \cdot 10^{-5}$	$4{,}31 \cdot 10^{-5}$
^{131m}Te	$6{,}08 \cdot 10^{-3}$	$5{,}50 \cdot 10^{-3}$	$4{,}88 \cdot 10^{-3}$	$4{,}51 \cdot 10^{-3}$	$3{,}93 \cdot 10^{-3}$	$3{,}30 \cdot 10^{-3}$	$2{,}40 \cdot 10^{-3}$	$1{,}74 \cdot 10^{-3}$
^{132}Te	$1{,}29 \cdot 10^{-3}$	$1{,}07 \cdot 10^{-3}$	$8{,}97 \cdot 10^{-4}$	$8{,}05 \cdot 10^{-4}$	$6{,}75 \cdot 10^{-4}$	$5{,}44 \cdot 10^{-4}$	$3{,}75 \cdot 10^{-4}$	$2{,}59 \cdot 10^{-4}$
^{131}I	$1{,}74 \cdot 10^{-3}$	$1{,}57 \cdot 10^{-3}$	$1{,}39 \cdot 10^{-3}$	$1{,}29 \cdot 10^{-3}$	$1{,}12 \cdot 10^{-3}$	$9{,}32 \cdot 10^{-4}$	$6{,}70 \cdot 10^{-4}$	$4{,}79 \cdot 10^{-4}$
^{132}I	$9{,}88 \cdot 10^{-3}$	$8{,}94 \cdot 10^{-3}$	$7{,}95 \cdot 10^{-3}$	$7{,}35 \cdot 10^{-3}$	$6{,}42 \cdot 10^{-3}$	$5{,}38 \cdot 10^{-3}$	$3{,}92 \cdot 10^{-3}$	$2{,}84 \cdot 10^{-3}$
^{133}I	$2{,}72 \cdot 10^{-3}$	$2{,}46 \cdot 10^{-3}$	$2{,}18 \cdot 10^{-3}$	$2{,}01 \cdot 10^{-3}$	$1{,}76 \cdot 10^{-3}$	$1{,}47 \cdot 10^{-3}$	$1{,}06 \cdot 10^{-3}$	$7{,}66 \cdot 10^{-4}$
^{134}I	$1{,}11 \cdot 10^{-2}$	$1{,}00 \cdot 10^{-2}$	$8{,}93 \cdot 10^{-3}$	$8{,}26 \cdot 10^{-3}$	$7{,}21 \cdot 10^{-3}$	$6{,}05 \cdot 10^{-3}$	$4{,}41 \cdot 10^{-3}$	$3{,}21 \cdot 10^{-3}$
^{134}Cs	$6{,}85 \cdot 10^{-3}$	$6{,}19 \cdot 10^{-3}$	$5{,}50 \cdot 10^{-3}$	$5{,}09 \cdot 10^{-3}$	$4{,}44 \cdot 10^{-3}$	$3{,}72 \cdot 10^{-3}$	$2{,}70 \cdot 10^{-3}$	$1{,}95 \cdot 10^{-3}$
^{136}Cs	$9{,}08 \cdot 10^{-3}$	$8{,}22 \cdot 10^{-3}$	$7{,}30 \cdot 10^{-3}$	$6{,}75 \cdot 10^{-3}$	$5{,}90 \cdot 10^{-3}$	$4{,}94 \cdot 10^{-3}$	$3{,}60 \cdot 10^{-3}$	$2{,}61 \cdot 10^{-3}$
^{137m}Ba	$2{,}68 \cdot 10^{-3}$	$2{,}42 \cdot 10^{-3}$	$2{,}15 \cdot 10^{-3}$	$1{,}98 \cdot 10^{-3}$	$1{,}73 \cdot 10^{-3}$	$1{,}44 \cdot 10^{-3}$	$1{,}05 \cdot 10^{-3}$	$7{,}55 \cdot 10^{-4}$
^{140}Ba	$9{,}32 \cdot 10^{-4}$	$7{,}86 \cdot 10^{-4}$	$6{,}79 \cdot 10^{-4}$	$6{,}21 \cdot 10^{-4}$	$5{,}35 \cdot 10^{-4}$	$4{,}42 \cdot 10^{-4}$	$3{,}16 \cdot 10^{-4}$	$2{,}25 \cdot 10^{-4}$
^{140}La	$9{,}27 \cdot 10^{-3}$	$8{,}39 \cdot 10^{-3}$	$7{,}47 \cdot 10^{-3}$	$6{,}93 \cdot 10^{-3}$	$6{,}06 \cdot 10^{-3}$	$5{,}10 \cdot 10^{-3}$	$3{,}75 \cdot 10^{-3}$	$2{,}75 \cdot 10^{-3}$
^{141}Ce	$3{,}67 \cdot 10^{-4}$	$3{,}13 \cdot 10^{-4}$	$2{,}69 \cdot 10^{-4}$	$2{,}44 \cdot 10^{-4}$	$2{,}09 \cdot 10^{-4}$	$1{,}68 \cdot 10^{-4}$	$1{,}15 \cdot 10^{-4}$	$7{,}82 \cdot 10^{-5}$
^{143}Ce	$1{,}39 \cdot 10^{-3}$	$1{,}19 \cdot 10^{-3}$	$1{,}02 \cdot 10^{-3}$	$9{,}28 \cdot 10^{-4}$	$7{,}90 \cdot 10^{-4}$	$6{,}45 \cdot 10^{-4}$	$4{,}53 \cdot 10^{-4}$	$3{,}20 \cdot 10^{-4}$
^{144}Ce	$1{,}08 \cdot 10^{-4}$	$8{,}70 \cdot 10^{-5}$	$7{,}17 \cdot 10^{-5}$	$6{,}37 \cdot 10^{-5}$	$5{,}27 \cdot 10^{-5}$	$4{,}13 \cdot 10^{-5}$	$2{,}72 \cdot 10^{-5}$	$1{,}80 \cdot 10^{-5}$

G.3 Factor $f_{H^*(10)}$ to convert activity to ambient dose equivalent rate for some relevant radionuclides at different relaxation masses per unit area, β[10]

Table G.3 contains the factors to convert the activity to ambient dose equivalent rate at 1 m above ground for some relevant radionuclides at different relaxation masses per unit area, β.

Table G.3 — Factors to convert the activity of unit of mass in ambient dose equivalent rate $\dot{H}^*(10)$ at 1 m above ground for different relaxation masses per unit area, β[10]1

		Conversion factor $f_{\dot{H}^*(10)}$ in nSv·m^2·h^{-1}·Bq^{-1} for relaxation mass per unit area β in kg·m^{-2}							
Radionuclide	nSv h^{-1} Bq^{-1}	nSv·m^2·h^{-1}·Bq^{-1}							nSv h^{-1} Bq^{-1} kg
	point source	exponential distribution							Homogen
		β = 0	β = 3	β = 10	β = 50	β = 100	β = 200	β = 500	($\beta \to \infty$)
Natural radionuclides or Natural radioactive series									
^{232}Th series (total)[2]	3,49 · 10^{-4}	1,19 · 10^{-2}	9,73 · 10^{-3}	7,79 · 10^{-3}	4,80 · 10^{-3}	3,51 · 10^{-3}	2,37 · 10^{-3}	1,25 · 10^{-3}	7,94 · 10^{-1}
^{208}Tl	4,18 · 10^{-4}	1,48 · 10^{-2}	1,22 · 10^{-2}	9,79 · 10^{-3}	6,14 · 10^{-3}	4,57 · 10^{-3}	3,16 · 10^{-3}	1,71 · 10^{-3}	1,12 · 10^{0}
^{228}Ac	1,50 · 10^{-4}	4,99 · 10^{-3}	4,04 · 10^{-3}	3,23 · 10^{-3}	1,97 · 10^{-3}	1,42 · 10^{-3}	9,47 · 10^{-4}	4,93 · 10^{-4}	3,06 · 10^{-1}
^{212}Pb	2,89 · 10^{-5}	9,81 · 10^{-4}	7,79 · 10^{-4}	6,23 · 10^{-4}	3,63 · 10^{-4}	2,54 · 10^{-4}	1,61 · 10^{-4}	7,84 · 10^{-5}	4,52 · 10^{-2}
^{212}Bi	1,71 · 10^{-5}	5,42 · 10^{-4}	4,38 · 10^{-4}	3,48 · 10^{-4}	2,17 · 10^{-4}	1,58 · 10^{-4}	1,06 · 10^{-4}	5,51 · 10^{-5}	3,41 · 10^{-2}
^{224}Ra	1,87 · 10^{-6}	6,65 · 10^{-5}	5,36 · 10^{-5}	4,33 · 10^{-5}	2,61 · 10^{-5}	1,87 · 10^{-5}	1,20 · 10^{-5}	5,90 · 10^{-6}	3,44 · 10^{-3}
^{238}U series (total)[2]	2,46 · 10^{-4}	8,45 · 10^{-3}	6,92 · 10^{-3}	5,61 · 10^{-3}	3,47 · 10^{-3}	2,53 · 10^{-3}	1,70 · 10^{-3}	8,86 · 10^{-4}	5,53 · 10^{-1}
^{214}Bi	2,00 · 10^{-4}	6,89 · 10^{-3}	5,67 · 10^{-3}	4,60 · 10^{-3}	2,86 · 10^{-3}	2,10 · 10^{-3}	1,42 · 10^{-3}	7,47 · 10^{-4}	4,72 · 10^{-1}
^{214}Pb	4,43 · 10^{-5}	1,51 · 10^{-3}	1,21 · 10^{-3}	9,78 · 10^{-4}	5,90 · 10^{-4}	4,18 · 10^{-4}	2,71 · 10^{-4}	1,35 · 10^{-4}	7,90 · 10^{-2}
^{226}Ra	1,45 · 10^{-6}	4,88 · 10^{-5}	3,93 · 10^{-5}	3,11 · 10^{-5}	1,85 · 10^{-5}	1,29 · 10^{-5}	8,09 · 10^{-6}	3,96 · 10^{-6}	2,26 · 10^{-3}
^{7}Be	8,40 · 10^{-6}	2,93 · 10^{-4}	2,37 · 10^{-4}	1,94 · 10^{-4}	1,19 · 10^{-4}	8,59 · 10^{-5}	5,63 · 10^{-5}	2,85 · 10^{-5}	1,70 · 10^{-2}
^{40}K	2,12 · 10^{-5}	7,27 · 10^{-4}	5,92 · 10^{-4}	4,88 · 10^{-4}	2,98 · 10^{-4}	2,22 · 10^{-4}	1,51 · 10^{-4}	8,06 · 10^{-5}	5,17 · 10^{-2}

"to be continued"

	Radionuclide	nSv·h^{-1}·Bq^{-1}	nSv·m^{2}·h^{-1}·Bq^{-1}							nSv·h^{-1}·Bq^{-1}·kg
		Point source	Exponential distribution							Homogen
			$\beta = 0$	$\beta = 3$	$\beta = 10$	$\beta = 50$	$\beta = 100$	$\beta = 200$	$\beta = 500$	($\beta \rightarrow \infty$)
Artificial radionuclides	^{51}Cr	$5{,}45 \cdot 10^{-6}$	$1{,}95 \cdot 10^{-4}$	$1{,}58 \cdot 10^{-4}$	$1{,}29 \cdot 10^{-4}$	$7{,}94 \cdot 10^{-5}$	$5{,}68 \cdot 10^{-5}$	$3{,}70 \cdot 10^{-5}$	$1{,}84 \cdot 10^{-5}$	$1{,}08 \cdot 10^{-2}$
	^{54}Mn	$1{,}30 \cdot 10^{-4}$	$4{,}42 \cdot 10^{-3}$	$3{,}64 \cdot 10^{-3}$	$2{,}88 \cdot 10^{-3}$	$1{,}81 \cdot 10^{-3}$	$1{,}31 \cdot 10^{-3}$	$8{,}76 \cdot 10^{-4}$	$4{,}56 \cdot 10^{-4}$	$2{,}83 \cdot 10^{-1}$
	^{57}Co	$2{,}27 \cdot 10^{-5}$	$7{,}94 \cdot 10^{-4}$	$6{,}41 \cdot 10^{-4}$	$5{,}16 \cdot 10^{-4}$	$3{,}03 \cdot 10^{-4}$	$2{,}06 \cdot 10^{-4}$	$1{,}28 \cdot 10^{-4}$	$6{,}09 \cdot 10^{-5}$	$3{,}33 \cdot 10^{-2}$
	^{58}Co	$1{,}54 \cdot 10^{-4}$	$5{,}27 \cdot 10^{-3}$	$4{,}32 \cdot 10^{-3}$	$3{,}43 \cdot 10^{-3}$	$2{,}14 \cdot 10^{-3}$	$1{,}56 \cdot 10^{-3}$	$1{,}04 \cdot 10^{-3}$	$5{,}36 \cdot 10^{-4}$	$3{,}29 \cdot 10^{-1}$
	^{60}Co	$3{,}54 \cdot 10^{-4}$	$1{,}21 \cdot 10^{-2}$	$9{,}92 \cdot 10^{-3}$	$8{,}08 \cdot 10^{-3}$	$4{,}96 \cdot 10^{-3}$	$3{,}65 \cdot 10^{-3}$	$2{,}50 \cdot 10^{-3}$	$1{,}30 \cdot 10^{-3}$	$8{,}25 \cdot 10^{-1}$
	^{59}Fe	$1{,}71 \cdot 10^{-4}$	$5{,}82 \cdot 10^{-3}$	$4{,}78 \cdot 10^{-3}$	$3{,}88 \cdot 10^{-3}$	$2{,}38 \cdot 10^{-3}$	$1{,}75 \cdot 10^{-3}$	$1{,}19 \cdot 10^{-3}$	$6{,}21 \cdot 10^{-4}$	$3{,}92 \cdot 10^{-1}$
	^{65}Zn	$8{,}41 \cdot 10^{-5}$	$2{,}87 \cdot 10^{-3}$	$2{,}36 \cdot 10^{-3}$	$1{,}90 \cdot 10^{-3}$	$1{,}17 \cdot 10^{-3}$	$8{,}57 \cdot 10^{-4}$	$5{,}84 \cdot 10^{-4}$	$3{,}02 \cdot 10^{-4}$	$1{,}89 \cdot 10^{-1}$
	^{95}Zr	$1{,}18 \cdot 10^{-4}$	$4{,}01 \cdot 10^{-3}$	$3{,}32 \cdot 10^{-3}$	$2{,}61 \cdot 10^{-3}$	$1{,}64 \cdot 10^{-3}$	$1{,}18 \cdot 10^{-3}$	$7{,}93 \cdot 10^{-4}$	$4{,}07 \cdot 10^{-4}$	$2{,}48 \cdot 10^{-1}$
	^{95}Nb	$1{,}21 \cdot 10^{-4}$	$4{,}15 \cdot 10^{-3}$	$3{,}42 \cdot 10^{-3}$	$2{,}69 \cdot 10^{-3}$	$1{,}69 \cdot 10^{-3}$	$1{,}22 \cdot 10^{-3}$	$8{,}19 \cdot 10^{-4}$	$4{,}22 \cdot 10^{-4}$	$2{,}58 \cdot 10^{-1}$
	^{99m}Tc	$2{,}35 \cdot 10^{-5}$	$8{,}35 \cdot 10^{-4}$	$6{,}70 \cdot 10^{-4}$	$5{,}39 \cdot 10^{-4}$	$3{,}20 \cdot 10^{-4}$	$2{,}20 \cdot 10^{-4}$	$1{,}38 \cdot 10^{-4}$	$6{,}60 \cdot 10^{-5}$	$3{,}63 \cdot 10^{-2}$
	^{110m}Ag	$4{,}21 \cdot 10^{-4}$	$1{,}43 \cdot 10^{-2}$	$1{,}18 \cdot 10^{-2}$	$9{,}44 \cdot 10^{-3}$	$5{,}88 \cdot 10^{-3}$	$4{,}28 \cdot 10^{-3}$	$2{,}87 \cdot 10^{-3}$	$1{,}49 \cdot 10^{-3}$	$9{,}24 \cdot 10^{-1}$
	^{122}Sb	$7{,}26 \cdot 10^{-5}$	$2{,}49 \cdot 10^{-3}$	$2{,}05 \cdot 10^{-3}$	$1{,}65 \cdot 10^{-3}$	$1{,}02 \cdot 10^{-3}$	$7{,}37 \cdot 10^{-4}$	$4{,}88 \cdot 10^{-4}$	$2{,}48 \cdot 10^{-4}$	$1{,}49 \cdot 10^{-1}$
	^{124}Sb	$2{,}58 \cdot 10^{-4}$	$8{,}85 \cdot 10^{-3}$	$7{,}31 \cdot 10^{-3}$	$5{,}92 \cdot 10^{-3}$	$3{,}69 \cdot 10^{-3}$	$2{,}69 \cdot 10^{-3}$	$1{,}82 \cdot 10^{-3}$	$9{,}51 \cdot 10^{-4}$	$5{,}94 \cdot 10^{-1}$
	^{125}Sb	$8{,}73 \cdot 10^{-5}$	$2{,}72 \cdot 10^{-3}$	$2{,}09 \cdot 10^{-3}$	$1{,}64 \cdot 10^{-3}$	$9{,}90 \cdot 10^{-4}$	$7{,}09 \cdot 10^{-4}$	$4{,}66 \cdot 10^{-4}$	$2{,}35 \cdot 10^{-4}$	$1{,}40 \cdot 10^{-1}$
	^{123m}Te	$3{,}53 \cdot 10^{-5}$	$1{,}09 \cdot 10^{-3}$	$8{,}06 \cdot 10^{-4}$	$6{,}19 \cdot 10^{-4}$	$3{,}58 \cdot 10^{-4}$	$2{,}46 \cdot 10^{-4}$	$1{,}54 \cdot 10^{-4}$	$7{,}43 \cdot 10^{-5}$	$4{,}14 \cdot 10^{-2}$
	^{131}I	$6{,}57 \cdot 10^{-5}$	$2{,}29 \cdot 10^{-3}$	$1{,}87 \cdot 10^{-3}$	$1{,}51 \cdot 10^{-3}$	$9{,}30 \cdot 10^{-4}$	$6{,}64 \cdot 10^{-4}$	$4{,}35 \cdot 10^{-4}$	$2{,}18 \cdot 10^{-4}$	$1{,}29 \cdot 10^{-1}$
	^{134}Cs	$2{,}49 \cdot 10^{-4}$	$8{,}52 \cdot 10^{-3}$	$7{,}02 \cdot 10^{-3}$	$5{,}58 \cdot 10^{-3}$	$3{,}48 \cdot 10^{-3}$	$2{,}52 \cdot 10^{-3}$	$1{,}68 \cdot 10^{-3}$	$8{,}62 \cdot 10^{-4}$	$5{,}24 \cdot 10^{-1}$
	^{137}Cs	$9{,}25 \cdot 10^{-5}$	$3{,}12 \cdot 10^{-3}$	$2{,}60 \cdot 10^{-3}$	$2{,}05 \cdot 10^{-3}$	$1{,}28 \cdot 10^{-3}$	$9{,}19 \cdot 10^{-4}$	$6{,}15 \cdot 10^{-4}$	$3{,}12 \cdot 10^{-4}$	$1{,}88 \cdot 10^{-1}$
	^{140}Ba	$3{,}35 \cdot 10^{-5}$	$1{,}11 \cdot 10^{-3}$	$8{,}73 \cdot 10^{-4}$	$7{,}00 \cdot 10^{-4}$	$4{,}23 \cdot 10^{-3}$	$3{,}04 \cdot 10^{-4}$	$1{,}99 \cdot 10^{-4}$	$1{,}01 \cdot 10^{-4}$	$5{,}97 \cdot 10^{-2}$
	^{140}La	$3{,}24 \cdot 10^{-4}$	$1{,}11 \cdot 10^{-2}$	$9{,}09 \cdot 10^{-3}$	$7{,}44 \cdot 10^{-3}$	$4{,}61 \cdot 10^{-3}$	$3{,}39 \cdot 10^{-3}$	$2{,}28 \cdot 10^{-3}$	$1{,}21 \cdot 10^{-3}$	$7{,}67 \cdot 10^{-1}$

[1] Here, the relaxation mass per unit area β is shown in unit [kg·m^{-2}]. In contrast the unit [g·cm^{-2}] is used in [10] (Swiss recommendation) (1 g ·cm^{-2} = 10 kg·cm^{-2}).

[2] In case of decay chain the total factor is the summation of all factors of the relevant radionuclides of the decay chain under equilibrium condition.

G.4 Example

G.4.1 Measured activities

The following values are determined by an *in situ* gamma spectrometer:

^{134}Cs: $2{,}1 \cdot 10^{4}$ Bq · m^{-2}

^{137}Cs: $4{,}15 \cdot 10^4$ Bq · m^{-2}

^{40}K: 550 Bq · kg^{-1}

^{232}Th: 28 Bq · kg^{-1}

^{238}U: 56 Bq · kg^{-1}

Artificial radionuclides: In calculating the dose rate, an exponential distribution of ^{134}Cs and ^{137}Cs in soil with relaxation mass per unit area β of 10 kg · m^{-2} is assumed.

Natural radionuclides: For ^{232}Th and ^{238}U and their daughters, homogeneous distribution in soil and radioactive equilibrium is assumed.

G.4.2 Calculation of the individual contribution to the air kerma rate

Individual contributions of the air kerma rate are calculated using Formula (18):

$$\dot{D}_{V,N} = f_D \cdot a$$

where

f_D is the factor to calculate the activity per unit of mass or surface area as air kerma rate nGy · m^2 · h^{-1} · Bq^{-1} or nGy · kg · h^{-1} · Bq^{-1};

a is the activity of the concerning radionuclides in Bq · m^{-2} or Bq · kg^{-1}.

The factors are taken from the tables in G.1 and G.2 and interpolated, if necessary. To determine the ambient dose rate for ^{137}Cs, the factor f_D of ^{137}mBa is used.

Results:

Individual contributions for relaxation mass per unit area, β, of 10 kg · m^{-2} for the artificial nuclides and values of $\beta \to \infty$ for homogeneous distribution for the natural nuclides result in the following:

^{134}Cs: $4{,}44 \cdot 10^{-3} \cdot 2{,}1 \cdot 10^4 = 93$ nGy · h^{-1}

^{137}Cs: $1{,}73 \cdot 10^{-3} \cdot 4{,}15 \cdot 10^4 = 72$ nGy · h^{-1}

^{40}K: $4{,}17 \cdot 10^{-2} \cdot 550 = 23$ nGy · h^{-1}

^{232}Th: $6{,}04 \cdot 10^{-1} \cdot 28 = 17$ nGy · h^{-1}

^{238}U: $4{,}62 \cdot 10^{-1} \cdot 56 = 26$ nGy · h^{-1}

Total ambient dose rate (air kerma rate): 231 nGy · h^{-1}

G.4.3 Calculation of the individual contribution to the ambient dose equivalent rate

Individual contributions of the ambient dose equivalent rate are calculated with Formula (19):

$$\dot{H}^{*}(10)_{V,N} = f_{\dot{H}^{*}(10)} \cdot a$$

where

$f_{\dot{H}^{*}(10)}$ is the factor to calculate the activity per unit of mass or surface area as ambient dose equivalent rate for natural radionuclides nSv · m^{2} · h-1 · Bq^{-1} or nSv · kg · h^{-1} · Bq^{-1};

a is the activity of the concerning radionuclides in Bq · m^{-2} or Bq · kg^{-1}.

The factors are taken from Table G.2 in Annex G and interpolated, if necessary.

Results:

Individual contributions for relaxation mass per unit area, β, of 10 kg · m^{-2} for the artificial radionuclides and values of $\beta \to \infty$ for homogeneous distribution for the natural radionuclides result in the following:

^{134}Cs: $5{,}58 \cdot 10^{-3} \cdot 2{,}1 \cdot 10^{4} = 73$ nSv · h^{-1}

^{137}Cs: $2{,}05 \cdot 10^{-3} \cdot 4{,}15 \cdot 10^{4} = 53$ nSv · h^{-1}

^{40}K: $5{,}17 \cdot 10^{-2} \cdot 550 = 28$ nSv · h^{-1}

^{232}Th: $7{,}94 \cdot 10^{-1} \cdot 28 = 22$ nSv · h^{-1}

^{238}U: $5{,}53 \cdot 10^{-1} \cdot 56 = 31$ nSv · h^{-1}

Total (ambient dose equivalent rate $\dot{H}^{*}(10)$): 279 nSv · h^{-1}.

Annex H
(informative)

Mass attenuation factors for soil and attenuation factors for air as a function of photon energy and deviation of *G(E,V)* for different soil compositions

The attenuation coefficients used in this part of ISO 18589 are based on the following compositions (given in parts of mass):

— Soil: Al_2O_3 13,5 %; Fe_2O_3 4,5 %; SiO_2 67,5 %; CO_2 4,5 %; H_2O 10 %[8]

— Air: CO_2 0,058 %; N_2 75,52 %; O_2 23,14 %; Ar 1,29 %; density 1,293 [kg·m^{-3}]

The graph in Figure H.1 shows the mass attenuation coefficient[12] for soil and the attenuation coefficient for air.

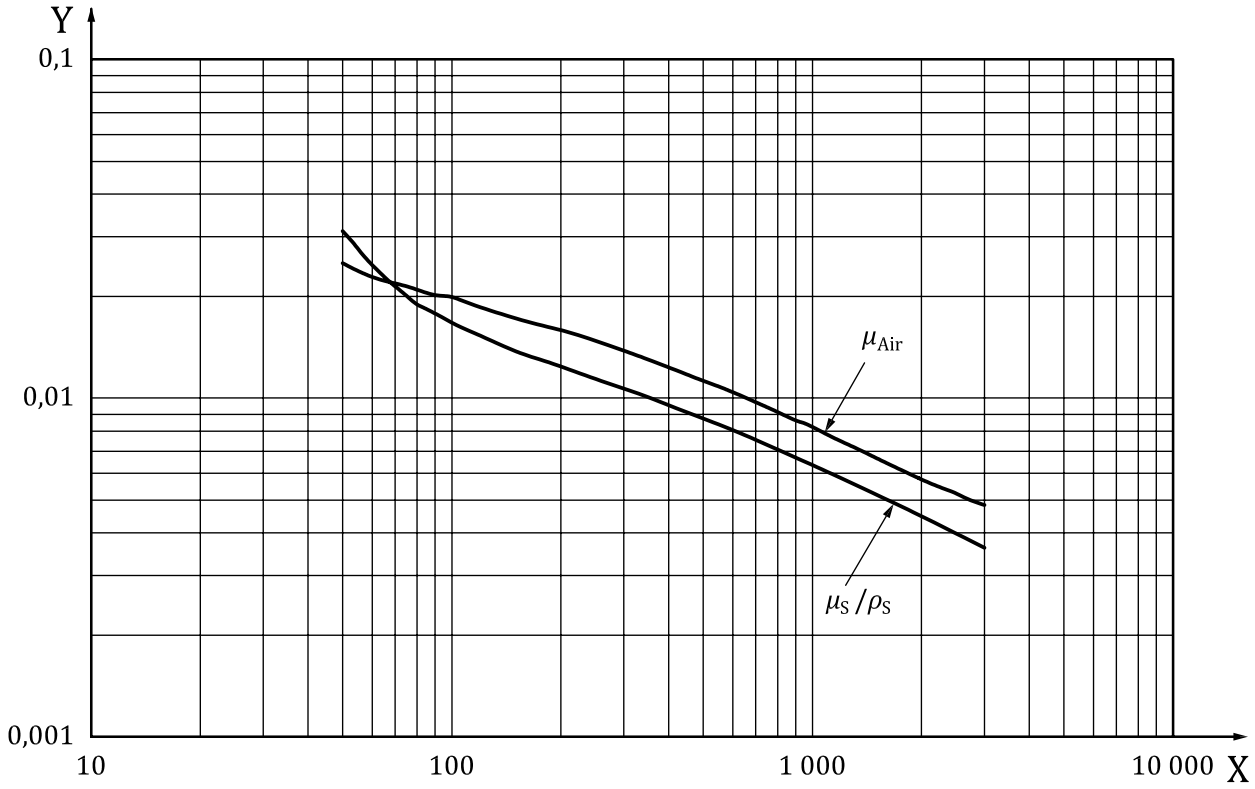

Key

X E in keV

Y μ_S/ρ_S in m^2·kg^{-1} and μ_{Air} in m^{-1}

Figure H.1 — Mass attenuation factors μ_S/ρ_S for soil and attenuation μ_{Air} factors for air as a function of photon energy

The attenuation coefficients used in Reference[7] are based on the following compositions (given in parts of mass):

— Soil: Al_2O_3 H 2,2 %; O 57,5 %; Al 8,5 %; Si 26,2 %; Fe 5,6 %

— Air: unknown

The deviation of $G(E,V)$ due to the different soil compositions of [7] and [8] is shown in Figure H.2.

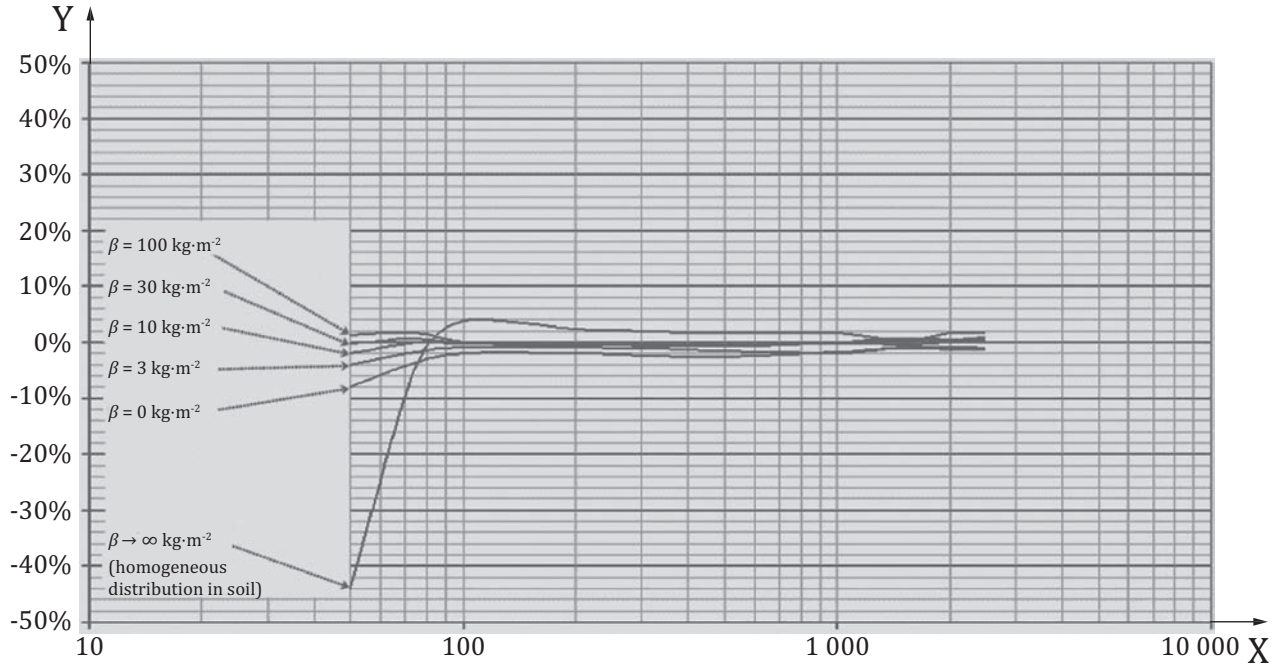

Key

X E in keV

Y ratio $(G(E,V)_{[8]} - G(E,V)_{[7]}) / G(E,V)_{[8]}$

Figure H.2 — Ratio of the geometry function $G(E, V)$ for ISO and ICRU soil compositions

For $\beta = 0$, $G(E,V)$ is independent of the soil composition as there is no interaction with the soil. The observed deviation for $\beta = 0$ could be caused by the difference of the composition and the density of the air.

Bibliography

[1] Debertin K., & Helmer R.G. *Gamma- and x-Ray spectrometry with semi-conductor detectors*. North Holland, 1988

[2] PTB-Ra-16/5 U. Schötzig und H. Schrader: Halbwertszeiten und Photonen-Emissionswahrscheinlichkeiten von häufig verwendeten Radionukliden, 5. erweiterte und korrigierte Auflage, Braunschweig (Mai 2000)

[3] CETAMA. *Spectrométrie gamma appliquée aux échantillons de l'environnement. Dossier de recommandations pour l'optimisation des mesures*. Editions TEC&DOC, Paris, 2002

[4] Hubbell J.H. Photon Mass Attenuation and Energy-Absorption Coefficient from 1 keV to 20 MeV. *Int. J. Appl. Radiat. Isot.* 1982, **33** pp. 1269–1290

[5] Selzer S.M. Calculation of Photon Mass Energy-Transfer and Mass Energy-Absorption Coefficients. *Radiat. Res.* 1993, **136** pp. 147–170

[6] Berger M.J., & Hubbell J.H. *Photon Cross Section on a Personal Computer; Publication NBSIR 87 - 3597*. National Institute of Standard, Gaithersburg, MD, 1987

[7] ICRU-Report 53, Gamma-Ray Spectrometry in the Environment, International Commission on Radiation Units and Measurements, 1994

[8] Beck H.L., DeCampo J., Gogolak C.In Situ Ge(Li) and Nal(TI) Gamma-Ray Spectrometry, Report HASL-258, U.S. Department of Energy, Environmental Measurements Laboratory, New York, 1972

[9] Lemercier M., Gurriaran R., Bouisset P., Cagnat X. Specific activity to H*(10) conversion Coefficients for in situ gamma spectrometry. *Radiat. Prot. Dosimetry*. 2008, **128** (1) pp. 83–89

[10] Commission fédérale de Protection contre les radiations et de surveillance de la Radioactivité Recommendation concerning the use of the factor h*(10) by measuring of ambient dose equivalent rate H*(10) with situ gamma spectrometry. Secrétariat scientifique KSR/CPR, Office fédéral de la santé publique, 3003 Bern, 25 janvier 2010

[11] Knoll G.F. *Radiation detection and measurement*. Wiley and Sons, New York, Fourth Edition, 2010

[12] National Institute of Standards and Technology. Physical measurement laboratory:XCOM: Photon Cross Sections Database. Available from: http://www.nist.gov/pml/data/xcom/index.cfm

[13] Winkelmann I., Haimerl W., Wutz J. *Nuklidspezifische Messungen der Ortsdosisleistung in der Umgebung kerntechnischer Anlagen, ISH-Bericht 12 des Bundesgesundheitsamtes*. Dezember, 1982

[14] Laedermann J.-P., Byrde F., Murith C. In-Situ Gamma-ray Spectrometry, the Influence of Topography on the Accuracy of Activity Determination. *J. Environ. Radioact.* 1998, **38** (1) pp. 1–16

[15] ISO/IEC Guide 98-3, *Uncertainty of measurement — Part 3: Guide to the expression of uncertainty in measurement (GUM:1995)*

[16] ISO 18589-1, *Measurement of radioactivity in the environment — Soil — Part 1: General guidelines and definitions*

[17] ISO 18589-2, *Measurement of radioactivity in the environment — Soil — Part 2: Guidance for the selection of the sampling strategy, sampling and pre-treatment of samples*

[18] ISO 18589-3, *Measurement of radioactivity in the environment — Soil — Part 3: Measurement of gamma-emitting radionuclides*

ICS 17.240;13.080.01

Price based on 54 pages